

Flow in a tube with non-uniform, time-dependent curvature: governing equations and simple examples

By D. G. LYNCH, S. L. WATERS AND T. J. PEDLEY†

Department of Applied Mathematical Studies, University of Leeds, Leeds, LS2 9JT, UK

(Received 8 February 1996 and revised form 7 May 1996)

Motivated by the study of blood flow in the major coronary arteries, which are situated on the outer surface of the pumping heart, we analyse flow of an incompressible Newtonian fluid in a tube whose curvature varies both along the tube and with time. Attention is restricted to the case in which the tube radius is fixed and its centreline moves in a plane. Nevertheless, the governing equations are very complicated, because the natural coordinate system involves acceleration, rotation and deformation of the frame of reference, and their derivation forms a major part of the paper. Then they are applied to two particular, relatively simple examples: a tube of uniform but time-dependent curvature; and a sinuous tube, representing a small-amplitude oscillation about a straight pipe. In the former case the curvature is taken to be small and to vary by a small amount, and the solution is developed as a triple power series in mean curvature ratio δ_0 , curvature variation ϵ and Dean number D . In the latter case the Reynolds number is taken to be large and a linearized solution for the perturbation to the flow in the boundary layer at the tube wall is obtained, following Smith (1976*a*). In each case the solution is taken far enough that the first non-trivial effects of the variable curvature can be determined. Results are presented in terms of the oscillatory wall shear stress distribution and, in the uniform curvature case, the contribution of steady streaming to the mean wall shear stress is calculated. Estimation of the parameters for the human heart indicates that the present results are not directly applicable, but point the way for future work.

1. Introduction

The flow of a viscous fluid in a curved tube is a classical problem in fluid dynamics with both technological and, especially, physiological applications. The main physiological application is to blood flow in arteries, because they are curved (and branched) and the distribution of atherosclerosis appears to be correlated with some measure of the time-dependent viscous wall shear stress exerted on the artery wall by the flowing blood, especially in the vicinity of geometric complexities, curves and branches, which vary from subject to subject. The mean value of wall shear stress has an influence on many factors in arterial endothelial cells, notably their mass transport properties and their production of chemicals such as nitric oxide, which are involved in atherosclerosis (Davies 1995). Fluctuations in wall shear stress are

† Present address: Department of Applied Mathematics and Theoretical Physics, University of Cambridge, Silver Street, Cambridge CB3 9EW, UK

also known to be important; see Friedman (1993), Giddens, Zarins & Glagov (1993), Pedley (1995) for recent review articles. A full assessment of 'geometrical risk factors' requires the ability to calculate the time-dependent wall shear stress at the relevant sites. The major coronary arteries are important sites for atherosclerosis because it can lead to heart attacks. However, a significant difficulty in predicting wall shear stress in these arteries comes from the fact that they are embedded in the surface of the heart, and therefore their overall geometry, represented by the curvature and torsion of the vessel centreline, as well as the diameter and length, changes with time during the cardiac cycle (Pao, Lu & Ritman 1992; see also figure 1). It is the purpose of this paper to begin to investigate the mechanics of flow in such time-dependent vessels.

The first theoretical description of steady flow in a uniform curved tube was by Dean (1927, 1928), who noted that, when the curvature ratio δ_0 ($= a/R$ where a is the tube radius and R is the radius of curvature of the centreline) is small, fully developed flow depends only on a single parameter D_0 , proportional to the product of the Reynolds number and $\delta_0^{1/2}$. This parameter is now called the Dean number. Dean himself calculated the velocity and pressure fields as series in powers of D_0 , the leading term being Poiseuille flow and the first correction incorporating secondary motions in the form of a pair of vortices, carrying flow across the centre of the tube to the outside of the curve, and back again near the walls. At larger values of D_0 the flow must be computed numerically, and the value of D_0 at which successful solutions have been computed has been increasing. Good early computations were provided by McConalogue & Srivastava (1968) and Collins & Dennis (1975) who took the two-vortex solution up to $D_0 = 600$ and $D_0 = 5000$ respectively. Among the most interesting recent results are those of Daskopoulos & Lenhoff (1989) who showed that the equations for steady fully-developed flow, in the small- δ_0 limit, have several different four-vortex solutions for values of D_0 above a critical value, though only the two-vortex solution is stable (Yanase, Goto & Yamamoto 1989). This suggests that the dynamical system represented by curved tube flow is not a simple one, and that unsteady flow is likely to be quite complicated.

Fully developed unsteady flow in fixed uniform curved tubes, of small δ_0 , driven by a time-dependent pressure gradient has also received considerable theoretical attention. The pioneering analytical study by Lyne (1971) considered a sinusoidally oscillating pressure gradient, with zero mean, at sufficiently high values of the frequency, Ω , that the Stokes layer thickness $(\nu/\Omega)^{1/2}$ is small compared with the tube radius a . It is within the Stokes layer for the axial velocity that secondary motions are generated by the nonlinear 'centrifugal force' terms in the equations. These secondary motions have a non-zero mean which does not go to zero at the edge of the Stokes layer and therefore drives a (two-vortex) steady secondary streaming flow across the whole tube. The direction of the secondary streaming is opposite to that for steady Dean flow. Subsequent workers have superimposed a mean onto the oscillation in order to investigate how the two types of secondary motion interact (Smith 1975; Blennerhassett 1976). Blennerhassett also found non-uniqueness at certain parameter values.

Non-fully developed steady (and unsteady) flow has been examined, both in the forms of entry flow with a flat velocity profile, as from a large reservoir (e.g. Singh 1975; Yao & Berger 1975), and of flow entering from a straight pipe with a parabolic profile (Smith 1976*a*). Analytical solutions have predominated, since they provide a more fundamental understanding, but are being supplemented by numerical solutions

in parts of the parameter space that the analysis cannot reach. The literature on curved tube flow up to about 1980 was thoroughly reviewed by Pedley (1980, chapter 4) and by Berger, Talbot & Yao (1983).

An examination of figure 1 reveals that, if the branches are neglected, the major blood vessels have two principal forms: large tubes whose curvature is single-signed and varies relatively slowly with longitudinal position, and small undulating tubes whose curvature changes sign and varies over a shorter length scale. During the cardiac cycle, the radii of curvature will change, generally increasing during left ventricular filling; there are also torsion and length changes (Pao *et al.* 1992). It is the purpose of this paper to begin an examination of viscous flow in tubes whose centreline curvature varies with position and time. Torsion is neglected, the centreline is taken to be inextensible, the tube cross-section is taken to be circular with uniform radius independent of time, and points on the wall which at one instant lie in a plane perpendicular to the centreline at a point S_0 remain in that plane as S_0 moves and the plane rotates. Moreover the centreline is taken to lie in a constant plane. Nevertheless, the problem is very complicated because the natural transverse coordinate system at a given point on the centreline (S_0) is non-inertial, experiencing time-dependent translation and rotation. Thus the main aim of this paper is to establish the appropriate governing equations. This is done in §2. Then in §§3 and 4 we consider two simple limiting cases in which the equations can be greatly simplified but the new terms have a calculable effect: flow of constant flow rate (a) through a tube of uniform curvature which varies at low frequency (a not-quite-quasi-steady perturbation of Dean's solution) and (b) through a tube with small-amplitude, time-dependent undulations about a straight configuration (a perturbation to Poiseuille flow). In each case the focus will be on the main contributions to the time-dependent wall shear stress, and on any steady streaming which might arise. In the final section we discuss the solutions in the context of the original motivation, blood flow in coronary arteries.

2. Governing equations

We start from the vector form of the Navier–Stokes and continuity equations for an incompressible viscous fluid, written with respect to an inertial frame of reference:

$$\nabla \cdot \hat{\mathbf{u}}' = 0, \quad (2.1)$$

$$\left. \frac{\partial \hat{\mathbf{u}}'}{\partial \hat{t}} \right|_I + (\hat{\mathbf{u}}' \cdot \nabla) \hat{\mathbf{u}}' = -\frac{1}{\rho} \nabla \hat{p} + \nu \nabla^2 \hat{\mathbf{u}}'. \quad (2.2)$$

Here the variables have their usual meanings and are dimensional.

Because of the complex motion of the chosen frame of reference, we find it safer to make the coordinate transformation from first principles, without invoking classical results on motion in an accelerated and rotating frame of reference.

We define \hat{s} as the dimensional distance along the centreline from a specified origin, (\hat{r}, θ) as polar coordinates in the cross-sectional plane and \hat{t} as the dimensional time; the tube wall is at $\hat{r} = a$. The dimensional Cartesian coordinate system $(\hat{x}, \hat{y}, \hat{z}, \hat{t}')$, where the centreline moves in the (\hat{x}, \hat{y}) -plane, is then transformed into the curvilinear system $(\hat{r}, \theta, \hat{s}, \hat{t})$. We assume that the centreline of the tube is given by a known function

$$\hat{y}_0 = af(\hat{s}, \hat{t}), \quad (2.3)$$

where $\hat{\mathbf{x}}_0 = \hat{x}_0 \mathbf{e}_x + \hat{y}_0 \mathbf{e}_y$ is the Cartesian position vector of a general point S_0 on the



FIGURE 1. Coronary angiogram of a post-mortem human heart, fixed at diastolic in-vivo dimensions by pressure perfusion at 100 mmHg (courtesy of Professor W. A. Seed, Charing Cross and Westminster Medical School).

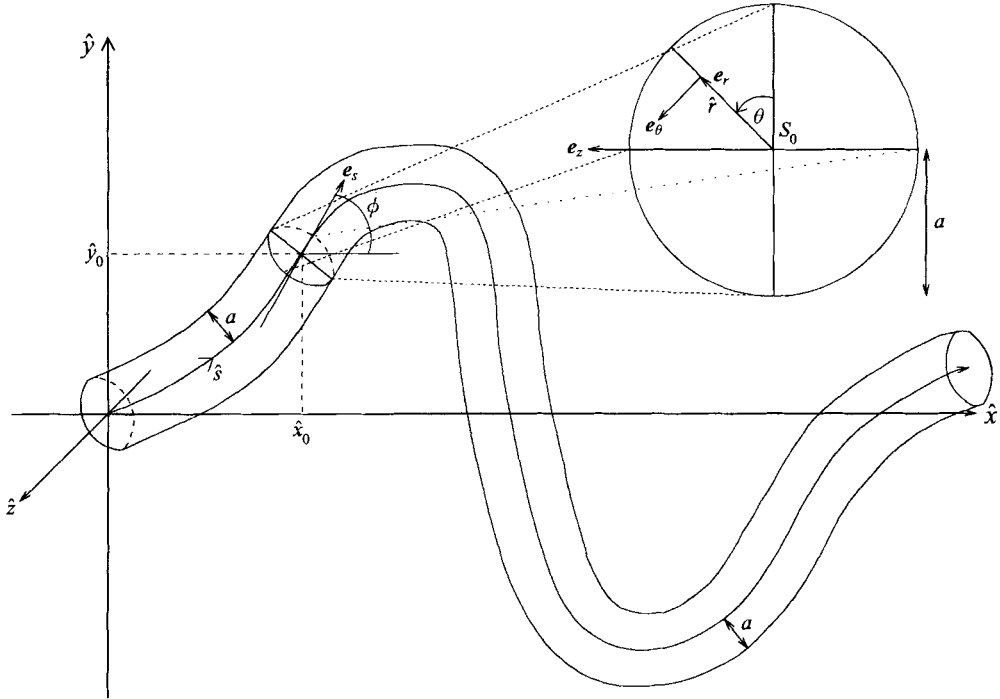


FIGURE 2. Diagram to show the time-dependent curvilinear coordinate system used to obtain the governing equations (general).

centreline (see figure 2). Then if ϕ is the angle between the tangent to the centreline at that point and the \hat{x} -axis we have

$$\hat{x} = \hat{x}_0 - \hat{r} \cos \theta \sin \phi, \quad \hat{y} = \hat{y}_0 + \hat{r} \cos \theta \cos \phi, \quad \hat{z} = \hat{r} \sin \theta, \quad \hat{t} = \hat{t}, \quad (2.4)$$

since $\hat{\mathbf{x}} = \hat{\mathbf{x}}_0 + \hat{r}\mathbf{e}_r$. The coordinate directions are related by

$$\left. \begin{aligned} \mathbf{e}_r &= -\mathbf{e}_x \sin \phi \cos \theta + \mathbf{e}_y \cos \phi \cos \theta + \mathbf{e}_z \sin \theta, \\ \mathbf{e}_\theta &= \mathbf{e}_x \sin \phi \sin \theta - \mathbf{e}_y \cos \phi \sin \theta + \mathbf{e}_z \cos \theta, \\ \mathbf{e}_s &= \mathbf{e}_x \cos \phi + \mathbf{e}_y \sin \phi \end{aligned} \right\} \quad (2.5)$$

or

$$\left. \begin{aligned} \mathbf{e}_x &= -\mathbf{e}_r \sin \phi \cos \theta + \mathbf{e}_\theta \sin \phi \sin \theta + \mathbf{e}_s \cos \phi, \\ \mathbf{e}_y &= \mathbf{e}_r \cos \phi \cos \theta - \mathbf{e}_\theta \cos \phi \sin \theta + \mathbf{e}_s \sin \phi, \\ \mathbf{e}_z &= \mathbf{e}_r \sin \theta + \mathbf{e}_\theta \cos \theta. \end{aligned} \right\} \quad (2.6)$$

Note that \mathbf{e}_r , \mathbf{e}_θ and \mathbf{e}_s are all dependent on \hat{r} , θ , \hat{s} and \hat{t} .

The functions $\hat{x}_0 = \hat{x}_0(\hat{s}, \hat{t})$ and $\phi = \phi(\hat{s}, \hat{t})$ need to be specified. Because \hat{y}_0 is a function only of \hat{s}, \hat{t} , it follows that

$$\left. \frac{\partial \hat{y}_0}{\partial \hat{x}_0} \right|_{\hat{t}} = \left. \frac{\partial \hat{y}_0}{\partial \hat{s}} \right|_{\hat{t}} \left. \frac{\partial \hat{s}}{\partial \hat{x}_0} \right|_{\hat{t}} = a f_s \left. \frac{\partial \hat{s}}{\partial \hat{x}_0} \right|_{\hat{t}},$$

where $f_s \equiv \partial f / \partial \hat{s}$. Also, at a given instant of time,

$$(\delta \hat{s})^2 = (\delta \hat{x}_0)^2 + (\delta \hat{y}_0)^2,$$

leading to

$$\left(\frac{\partial \hat{s}}{\partial \hat{x}_0} \Big|_{\hat{r}} \right)^2 = 1 + \left(\frac{\partial \hat{y}_0}{\partial \hat{x}_0} \Big|_{\hat{r}} \right)^2.$$

This gives

$$\frac{\partial \hat{x}_0}{\partial \hat{s}} \Big|_{\hat{r}} = \frac{\partial \hat{x}_0}{\partial \hat{s}} \Big|_{\hat{i}} = (1 - a^2 f_s^2)^{1/2} \equiv C_1(\hat{s}, \hat{t})$$

and hence

$$\hat{x}_0 = \int_0^{\hat{s}} C_1(\hat{s}', \hat{t}) d\hat{s}' \equiv aI(\hat{s}, \hat{t}). \tag{2.7}$$

Moreover, since

$$\tan \phi = \frac{\partial \hat{y}_0}{\partial \hat{x}_0} \Big|_{\hat{r}} = \frac{\partial \hat{y}_0}{\partial \hat{s}} \Big|_{\hat{i}} \frac{\partial \hat{s}}{\partial \hat{x}_0} \Big|_{\hat{r}} = a f_s C_1^{-1}$$

we have

$$\sin \phi = a f_s, \quad \cos \phi = C_1 \tag{2.8}$$

and hence from (2.4)

$$\hat{x} = aI - a f_s \hat{r} \cos \theta, \quad \hat{y} = a f_s + C_1 \hat{r} \cos \theta, \quad \hat{z} = \hat{r} \sin \theta. \tag{2.9}$$

To be able to convert the coordinate system $\hat{x}^i \equiv (\hat{x}, \hat{y}, \hat{z}, \hat{t})$ to $\hat{\zeta}^i \equiv (\hat{r}, \theta, \hat{s}, \hat{t})$, $i = 1 \dots 4$, we require the partial derivatives $\partial/\partial \hat{x}^i$ (e.g. $\partial/\partial \hat{x}|_{\hat{y}, \hat{z}, \hat{t}}$) in terms of the $\partial/\partial \hat{\zeta}^i$ (e.g. $\partial/\partial \hat{r}|_{\theta, \hat{s}, \hat{t}}$). Using (2.9) to find $\partial \hat{x}^j/\partial \hat{\zeta}^i$, $j = 1 \dots 3$, $i = 1 \dots 4$ and the chain rule on \hat{x}^j , $j = 1 \dots 3$ to obtain four sets of three simultaneous equations for $\partial \hat{\zeta}^j/\partial \hat{x}^i$, we obtain the required relations:

$$\left. \begin{aligned} \frac{\partial}{\partial \hat{x}} \Big|_{\hat{y}, \hat{z}, \hat{t}} &= -a f_s \cos \theta \frac{\partial}{\partial \hat{r}} \Big|_{\theta, \hat{s}, \hat{t}} + \frac{a}{\hat{r}} f_s \sin \theta \frac{\partial}{\partial \theta} \Big|_{\hat{r}, \hat{s}, \hat{t}} + C_1 h^{-1} \frac{\partial}{\partial \hat{s}} \Big|_{\hat{r}, \theta, \hat{t}}, \\ \frac{\partial}{\partial \hat{y}} \Big|_{\hat{x}, \hat{z}, \hat{t}} &= C_1 \cos \theta \frac{\partial}{\partial \hat{r}} \Big|_{\theta, \hat{s}, \hat{t}} - \frac{1}{\hat{r}} C_1 \sin \theta \frac{\partial}{\partial \theta} \Big|_{\hat{r}, \hat{s}, \hat{t}} + a f_s h^{-1} \frac{\partial}{\partial \hat{s}} \Big|_{\hat{r}, \theta, \hat{t}}, \\ \frac{\partial}{\partial \hat{z}} \Big|_{\hat{x}, \hat{y}, \hat{t}} &= \sin \theta \frac{\partial}{\partial \hat{r}} \Big|_{\theta, \hat{s}, \hat{t}} + \frac{1}{\hat{r}} \cos \theta \frac{\partial}{\partial \theta} \Big|_{\hat{r}, \hat{s}, \hat{t}}, \\ \frac{\partial}{\partial \hat{t}} \Big|_{\hat{x}, \hat{y}, \hat{z}} &= C_2 \cos \theta \frac{\partial}{\partial \hat{r}} \Big|_{\theta, \hat{s}, \hat{t}} - \frac{1}{\hat{r}} C_2 \sin \theta \frac{\partial}{\partial \theta} \Big|_{\hat{r}, \hat{s}, \hat{t}} \\ &\quad + h^{-1} C_1^{-1} [a f_s C_2 + a f_{\hat{s}\hat{t}} \hat{r} \cos \theta - a I_{\hat{t}}] \frac{\partial}{\partial \hat{s}} \Big|_{\hat{r}, \theta, \hat{t}} + \frac{\partial}{\partial \hat{t}} \Big|_{\hat{r}, \theta, \hat{s}}, \end{aligned} \right\} \tag{2.10}$$

where

$$C_2(\hat{s}, \hat{t}) = a^2 f_{\hat{s}} I_{\hat{t}} - a f_{\hat{t}} C_1 \tag{2.11}$$

and

$$h(\hat{r}, \theta, \hat{s}, \hat{t}) = 1 - a \hat{r} f_{\hat{s}\hat{s}} C_1^{-1} \cos \theta. \tag{2.12}$$

Note that $h \Delta \hat{s}$ is the displacement of a point when \hat{s} changes and \hat{r}, θ, \hat{t} do not. In transforming the vector operators that arise in (2.1) and (2.2), it is necessary

to consider changes in the coordinate directions (2.5) with $\hat{r}, \theta, \hat{s}, \hat{t}$. The relevant derivatives are

$$\left. \begin{aligned} \frac{\partial \mathbf{e}_r}{\partial \hat{r}} \Big|_{\theta, \hat{s}, \hat{t}} &= 0, & \frac{\partial \mathbf{e}_\theta}{\partial \hat{r}} \Big|_{\theta, \hat{s}, \hat{t}} &= 0, & \frac{\partial \mathbf{e}_s}{\partial \hat{r}} \Big|_{\theta, \hat{s}, \hat{t}} &= 0, \\ \frac{\partial \mathbf{e}_r}{\partial \theta} \Big|_{\hat{r}, \hat{s}, \hat{t}} &= \mathbf{e}_\theta, & \frac{\partial \mathbf{e}_\theta}{\partial \theta} \Big|_{\hat{r}, \hat{s}, \hat{t}} &= -\mathbf{e}_r, & \frac{\partial \mathbf{e}_s}{\partial \theta} \Big|_{\hat{r}, \hat{s}, \hat{t}} &= 0, \\ \frac{\partial \mathbf{e}_r}{\partial \hat{s}} \Big|_{\hat{r}, \theta, \hat{t}} &= -af_{\hat{s}\hat{s}}C_1^{-1} \cos \theta \mathbf{e}_s, & \frac{\partial \mathbf{e}_\theta}{\partial \hat{s}} \Big|_{\hat{r}, \theta, \hat{t}} &= af_{\hat{s}\hat{s}}C_1^{-1} \sin \theta \mathbf{e}_s, \\ \frac{\partial \mathbf{e}_s}{\partial \hat{s}} \Big|_{\hat{r}, \theta, \hat{t}} &= af_{\hat{s}\hat{s}}C_1^{-1} (\cos \theta \mathbf{e}_r - \sin \theta \mathbf{e}_\theta), & \frac{\partial \mathbf{e}_r}{\partial \hat{t}} \Big|_{\hat{r}, \theta, \hat{s}} &= -af_{\hat{s}\hat{t}}C_1^{-1} \cos \theta \mathbf{e}_s, \\ \frac{\partial \mathbf{e}_s}{\partial \hat{t}} \Big|_{\hat{r}, \theta, \hat{s}} &= af_{\hat{s}\hat{t}}C_1^{-1} (\cos \theta \mathbf{e}_r - \sin \theta \mathbf{e}_\theta), & \frac{\partial \mathbf{e}_\theta}{\partial \hat{t}} \Big|_{\hat{r}, \theta, \hat{s}} &= af_{\hat{s}\hat{t}}C_1^{-1} \sin \theta \mathbf{e}_s. \end{aligned} \right\} \quad (2.13)$$

Now, if we define $(\hat{u}', \hat{v}', \hat{w}')$ as being the dimensional velocity components in the $(\hat{r}, \theta, \hat{s})$ directions and \hat{p} as the dimensional pressure, and substitute (2.10) and (2.13) into (2.1) and (2.2), we obtain the continuity, \hat{r} -momentum, θ -momentum and \hat{s} -momentum equations as follows

$$\hat{u}'_r + \frac{1}{\hat{r}} \hat{v}'_\theta + h^{-1} \hat{w}'_s + \frac{1}{\hat{r}} \hat{u}' - af_{\hat{s}\hat{s}} h^{-1} C_1^{-1} (\cos \theta \hat{u}' - \sin \theta \hat{v}') = 0, \quad (2.14)$$

$$\begin{aligned} & \hat{u}'_t + \hat{u}' \hat{u}'_r + \frac{1}{\hat{r}} \hat{v}' \hat{u}'_\theta + h^{-1} \hat{w}' \hat{u}'_s - \frac{1}{\hat{r}} \hat{v}'^2 + af_{\hat{s}\hat{s}} C_1^{-1} \cos \theta h^{-1} \hat{w}'^2 \\ & + af_{\hat{s}\hat{t}} C_1^{-1} \cos \theta \hat{w}' + C_2 \cos \theta \hat{u}'_r - \frac{C_2}{\hat{r}} \sin \theta \hat{u}'_\theta + \frac{C_2}{\hat{r}} \sin \theta \hat{v}' \\ & + aC_1^{-1} h^{-1} [f_{\hat{s}} C_2 + \hat{r} f_{\hat{s}\hat{t}} \cos \theta - I_t] \{ \hat{u}'_s + af_{\hat{s}\hat{s}} C_1^{-1} \cos \theta \hat{w}' \} \\ = & -\frac{1}{\rho} \hat{p}_r + \nu \left\{ \frac{1}{\hat{r}^2} \hat{u}'_{\theta\theta} + h^{-2} \hat{u}'_{\hat{s}\hat{s}} - \frac{1}{\hat{r}} \hat{v}'_{r\theta} - \frac{1}{\hat{r}^2} \hat{v}'_\theta - h^{-1} \hat{w}'_{\hat{r}\hat{s}} \right. \\ & + af_{\hat{s}\hat{s}} C_1^{-1} \cos \theta h^{-2} \hat{w}'_s + aC_1^{-1} \cos \theta h^{-3} [f_{\hat{s}\hat{s}\hat{s}} + a^2 f_{\hat{s}} f_{\hat{s}\hat{s}}^2 C_1^{-2}] [\hat{w}' + \hat{r} \hat{u}'_s] \\ & \left. - af_{\hat{s}\hat{s}} C_1^{-1} \sin \theta h^{-1} \left(\hat{v}'_r - \frac{1}{\hat{r}} \hat{u}'_\theta + \frac{1}{\hat{r}} \hat{v}' \right) \right\}, \end{aligned} \quad (2.15)$$

$$\begin{aligned} & \hat{v}'_t + \hat{u}' \hat{v}'_r + \frac{1}{\hat{r}} \hat{v}' \hat{v}'_\theta + h^{-1} \hat{w}' \hat{v}'_s + \frac{1}{\hat{r}} \hat{u}' \hat{v}' - af_{\hat{s}\hat{s}} C_1^{-1} \sin \theta h^{-1} \hat{w}'^2 \\ & - af_{\hat{s}\hat{t}} C_1^{-1} \sin \theta \hat{w}' + C_2 \cos \theta \hat{v}'_r - \frac{C_2}{\hat{r}} \sin \theta \hat{v}'_\theta - \frac{C_2}{\hat{r}} \sin \theta \hat{u}' \\ & + aC_1^{-1} h^{-1} [f_{\hat{s}} C_2 + \hat{r} f_{\hat{s}\hat{t}} \cos \theta - I_t] \{ \hat{v}'_s - af_{\hat{s}\hat{s}} C_1^{-1} \sin \theta \hat{w}' \} \\ = & -\frac{1}{\rho \hat{r}} \hat{p}_\theta + \nu \left\{ \hat{v}'_{r\hat{r}} + h^{-2} \hat{v}'_{\hat{s}\hat{s}} - \hat{r}^{-1} h^{-1} \hat{w}'_{\theta\hat{s}} - \frac{1}{\hat{r}} \hat{u}'_{r\theta} + \hat{r}^{-2} h^{-1} \hat{u}'_\theta + \frac{1}{\hat{r}} \hat{v}'_r \right. \\ & - \hat{r}^{-2} h^{-1} \hat{v}' - ah^{-3} C_1^{-1} [f_{\hat{s}\hat{s}\hat{s}} + a^2 f_{\hat{s}} f_{\hat{s}\hat{s}}^2 C_1^{-2}] [\sin \theta \hat{w}' - \hat{r} \cos \theta \hat{v}'_s] \\ & \left. - af_{\hat{s}\hat{s}} C_1^{-1} h^{-1} (h^{-1} \sin \theta \hat{w}'_s + \cos \theta \hat{v}'_r) \right\}, \end{aligned} \quad (2.16)$$

$$\begin{aligned}
& \hat{w}'_i + \hat{u}'\hat{w}'_r + \frac{1}{\hat{r}}\hat{v}'\hat{w}'_\theta + h^{-1}\hat{w}'\hat{w}'_s - af_{ss}C_1^{-1}h^{-1}(\cos\theta\hat{u}' - \sin\theta\hat{v}')\hat{w}' \\
& - af_{st}C_1^{-1}(\cos\theta\hat{u}' - \sin\theta\hat{v}') + C_2\cos\theta\hat{w}'_r - \frac{C_2}{\hat{r}}\sin\theta\hat{w}'_\theta \\
& + aC_1^{-1}h^{-1}[f_sC_2 + \hat{r}f_{st}\cos\theta - I_i]\{\hat{w}'_s - af_{ss}C_1^{-1}(\cos\theta\hat{u}' - \sin\theta\hat{v}')\} \\
& = -\frac{1}{\rho h}\hat{p}_s + v\left\{\hat{w}'_{rr} + \frac{1}{\hat{r}^2}\hat{w}'_{\theta\theta} - h^{-1}\hat{u}'_{rs} - \hat{r}^{-1}h^{-2}\hat{u}'_s + \frac{1}{\hat{r}}\hat{w}'_r - \hat{r}^{-1}h^{-1}\hat{v}'_{\theta s}\right. \\
& \left. + af_{ss}C_1^{-1}h^{-1}\left(h^{-1}\sin\theta\hat{v}'_s + \frac{1}{\hat{r}}\sin\theta\hat{w}'_\theta - \cos\theta\hat{w}'_r\right) - a^2f_{ss}^2C_1^{-2}h^{-2}\hat{w}'\right\}, \tag{2.17}
\end{aligned}$$

where v is the kinematic viscosity of the fluid.

It should be noted in the above that \hat{u}' is the inertial velocity vector of the fluid, but it is written in terms of the new coordinate directions e_r, e_θ and e_s . It is non-zero on the boundary of the tube since no slip requires the fluid velocity to be equal to the velocity of the moving boundaries. Our aim is to formulate a system of velocity components that gives zero velocity on the boundaries. Firstly, therefore, we have to find the velocity of these moving boundaries. From our assumptions we know that a given point on the boundary $\hat{x}_B = \hat{x}_0 + ae_r$ has a fixed value of arclength \hat{s} as it moves around (although the position vector of the associated point on the centreline, \hat{x}_0 , does vary with time). Since $\hat{r} (= a)$ and θ are also constant with respect to time we can state that on the boundary

$$\frac{\partial}{\partial \hat{t}} \Big|_{\hat{r}, \theta, \hat{s}} = \frac{d}{dt}.$$

Hence for a boundary point,

$$\dot{\hat{x}}_B = a[f_iC_1 - af_sI_i]\{\cos\theta e_r - \sin\theta e_\theta\} - a[af_{st}C_1^{-1}\cos\theta - C_1I_i - af_{st}f_i]e_s. \tag{2.18}$$

If we also consider an internal point of the disc, $\hat{x}_D = \hat{x}_0 + \hat{r}e_r, \hat{r} \in [0, a]$, such that \hat{r}, θ and \hat{s} remain constant (i.e. there is no motion relative to the tube) then

$$\dot{\hat{x}}_D = a[f_iC_1 - af_sI_i]\{\cos\theta e_r - \sin\theta e_\theta\} - a[\hat{r}f_{st}C_1^{-1}\cos\theta - C_1I_i - af_{st}f_i]e_s. \tag{2.19}$$

Thus if we make the transformation

$$\hat{u}' = \hat{u} + \dot{\hat{x}}_D, \tag{2.20}$$

we have the much more convenient boundary condition of

$$\hat{u} = (\hat{u}, \hat{v}, \hat{w}) = \mathbf{0} \quad \text{on } \hat{r} = a. \tag{2.21}$$

Finally, therefore, substituting (2.20), with (2.19), into (2.14)–(2.17), we derive the complete new set of equations of motion:

continuity:

$$\begin{aligned}
& \hat{u}_r + \frac{1}{\hat{r}}\hat{v}_\theta + h^{-1}\hat{w}_s + \frac{1}{\hat{r}}\hat{u} \\
& - aC_1^{-1}h^{-1}(f_{ss}[\cos\theta\hat{u} - \sin\theta\hat{v}] + \hat{r}\cos\theta[f_{sst} + a^2f_s f_{ss} f_{st} C_1^{-2}]) = 0, \tag{2.22}
\end{aligned}$$

e_r :

$$\begin{aligned} & \hat{u}_\tau + \hat{u}\hat{u}_\tau + \frac{1}{\hat{r}}\hat{v}\hat{u}_\theta + h^{-1}\hat{w}\hat{u}_s - \frac{1}{\hat{r}}\hat{v}^2 + af_{\hat{s}\hat{s}}C_1^{-1}\cos\theta h^{-1}\hat{w}^2 \\ & + 2af_{\hat{s}\hat{t}}C_1^{-1}\cos\theta\hat{w} + a[f_{\hat{t}\hat{t}}C_1 - af_{\hat{s}}I_{\hat{t}\hat{t}}]\cos\theta - a^2\hat{r}f_{\hat{s}\hat{t}}^2C_1^{-2}\cos^2\theta \\ = & -\frac{1}{\rho}\hat{p}_\tau + v\left\{\frac{1}{\hat{r}^2}\hat{u}_{\theta\theta} + h^{-2}\hat{u}_{\hat{s}\hat{s}} - \frac{1}{\hat{r}}\hat{v}_{\hat{r}\theta} - af_{\hat{s}\hat{s}}C_1^{-1}h^{-1}\sin\theta\left(\hat{v}_{\hat{r}} - \frac{1}{\hat{r}}\hat{u}_\theta + \frac{1}{\hat{r}}\hat{v}\right)\right. \\ & - \frac{1}{\hat{r}^2}\hat{v}_\theta - h^{-1}\hat{w}_{\hat{r}\hat{s}} + aC_1^{-1}h^{-3}\cos\theta[f_{\hat{s}\hat{s}\hat{s}} + a^2f_{\hat{s}}f_{\hat{s}\hat{s}}^2C_1^{-2}][\hat{w} + \hat{r}\hat{u}_s] \\ & \left. + af_{\hat{s}\hat{s}}C_1^{-1}h^{-2}\cos\theta\hat{w}_s + 2ah^{-1}C_1^{-1}\cos\theta[f_{\hat{s}\hat{s}\hat{t}} + a^2f_{\hat{s}}f_{\hat{s}\hat{s}}f_{\hat{s}\hat{t}}C_1^{-2}]\right\}, \end{aligned} \quad (2.23)$$

e_θ :

$$\begin{aligned} & \hat{v}_\tau + \hat{u}\hat{v}_\tau + \frac{1}{\hat{r}}\hat{v}\hat{v}_\theta + h^{-1}\hat{w}\hat{v}_s + \frac{1}{\hat{r}}\hat{u}\hat{v} - af_{\hat{s}\hat{s}}C_1^{-1}\sin\theta h^{-1}\hat{w}^2 \\ & - 2af_{\hat{s}\hat{t}}C_1^{-1}\sin\theta\hat{w} - a[f_{\hat{t}\hat{t}}C_1 - af_{\hat{s}}I_{\hat{t}\hat{t}}]\sin\theta + a^2\hat{r}f_{\hat{s}\hat{t}}^2C_1^{-2}\sin\theta\cos\theta \\ = & -\frac{1}{\rho\hat{r}}\hat{p}_\theta + v\left\{\hat{v}_{\hat{r}\hat{r}} + h^{-2}\hat{v}_{\hat{s}\hat{s}} - \hat{r}^{-1}h^{-1}\hat{w}_{\theta s} - \frac{1}{\hat{r}}\hat{u}_{\hat{r}\theta} + \hat{r}^{-2}h^{-1}\hat{u}_\theta - \hat{r}^{-2}h^{-1}\hat{v}\right. \\ & - af_{\hat{s}\hat{s}}C_1^{-1}h^{-1}\cos\theta\hat{v}_{\hat{r}} - aC_1^{-1}h^{-3}[f_{\hat{s}\hat{s}\hat{s}} + a^2f_{\hat{s}}f_{\hat{s}\hat{s}}^2C_1^{-2}][\sin\theta\hat{w} - \hat{r}\cos\theta\hat{v}_s] \\ & \left. + \frac{1}{\hat{r}}\hat{v}_{\hat{r}} - af_{\hat{s}\hat{s}}C_1^{-1}h^{-2}\sin\theta\hat{w}_s - 2aC_1^{-1}h^{-1}\sin\theta[f_{\hat{s}\hat{s}\hat{t}} + a^2f_{\hat{s}}f_{\hat{s}\hat{s}}f_{\hat{s}\hat{t}}C_1^{-2}]\right\}, \end{aligned} \quad (2.24)$$

e_s :

$$\begin{aligned} & \hat{w}_\tau + \hat{u}\hat{w}_\tau + \frac{1}{\hat{r}}\hat{v}\hat{w}_\theta + h^{-1}\hat{w}\hat{w}_s - af_{\hat{s}\hat{s}}C_1^{-1}h^{-1}(\cos\theta\hat{u} - \sin\theta\hat{v})\hat{w} \\ & - 2af_{\hat{s}\hat{t}}C_1^{-1}(\cos\theta\hat{u} - \sin\theta\hat{v}) - a\hat{r}C_1^{-1}h^{-1}\cos\theta[f_{\hat{s}\hat{s}\hat{t}} + a^2f_{\hat{s}}f_{\hat{s}\hat{s}}f_{\hat{s}\hat{t}}C_1^{-2}]\hat{w} \\ & + a^2f_{\hat{s}}f_{\hat{t}\hat{t}} + aC_1I_{\hat{t}\hat{t}} - a\hat{r}C_1^{-1}\cos\theta[f_{\hat{s}\hat{t}\hat{t}} + a^2f_{\hat{s}}f_{\hat{s}\hat{t}}^2C_1^{-2}] \\ = & -\frac{1}{\rho h}\hat{p}_s + v\left\{\hat{w}_{\hat{r}\hat{r}} + \frac{1}{\hat{r}^2}\hat{w}_{\theta\theta} - h^{-1}\hat{u}_{\hat{r}\hat{s}} - \hat{r}^{-1}h^{-2}\hat{u}_s + \frac{1}{\hat{r}}\hat{w}_{\hat{r}} - \hat{r}^{-1}h^{-1}\hat{v}_{\theta s}\right. \\ & \left. + af_{\hat{s}\hat{s}}C_1^{-1}h^{-1}\left(h^{-1}\sin\theta\hat{v}_s + \frac{1}{\hat{r}}\sin\theta\hat{w}_\theta - \cos\theta\hat{w}_{\hat{r}}\right) - a^2f_{\hat{s}\hat{s}}^2C_1^{-2}h^{-2}\hat{w}\right\}. \end{aligned} \quad (2.25)$$

In many ways equations (2.23)–(2.25) are simpler than the corresponding equations (2.15)–(2.17). Most of the inertia terms linear in the unknown velocity components have been eliminated by the transformation (2.20). The remaining terms on the left-hand sides of the \hat{r} - and θ -equations, (2.23) and (2.24), are essentially the same as for steady flow except for the terms involving $f_{\hat{s}\hat{t}}\hat{w}$ which is a ‘Coriolis force’ associated with rotation of the frame of reference, terms involving $\hat{r}f_{\hat{s}\hat{t}}^2$, representing ‘centrifugal force’, and terms involving $f_{\hat{t}\hat{t}}$ and $I_{\hat{t}\hat{t}}$, which correspond to acceleration of the frame of reference. Similarly in the \hat{s} -equation (2.25), the $f_{\hat{s}\hat{t}}(\hat{u}, \hat{v})$ terms are ‘Coriolis force’, the $\hat{r}f_{\hat{s}\hat{t}}^2$ terms are ‘centrifugal force’, and the $f_{\hat{t}\hat{t}}$, $I_{\hat{t}\hat{t}}$ and $\hat{r}f_{\hat{s}\hat{t}\hat{t}}$ terms represent acceleration of the frame of reference. The additional ‘new’ inertia term is the one linear in \hat{w} at the end of the second line of (2.25); this cannot be simply attributed to any of the classical ‘forces’ seen in the systems translating and rotating with uniform acceleration and angular velocity, and represents spatial variation in these quantities. The new, intrinsically unsteady, terms on the right-hand sides of (2.23) and (2.24) are viscous terms associated with the deformation of the frame of reference velocity \hat{x}_D (equation

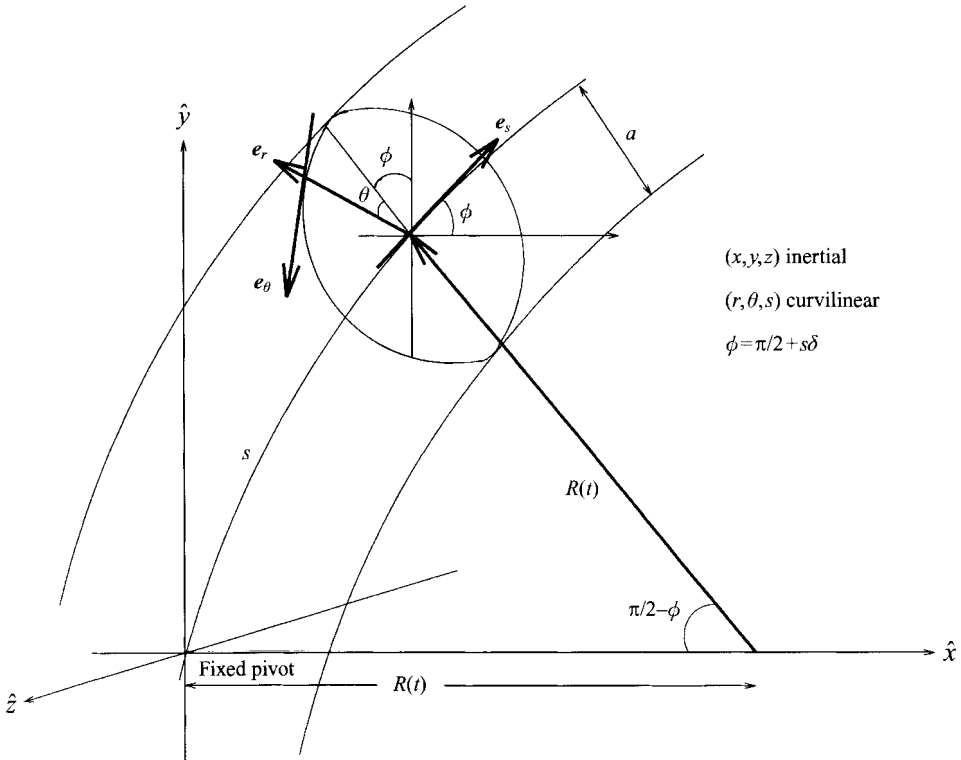


FIGURE 3. Diagram to show the time-dependent curvilinear coordinate system used to obtain the governing equations (uniform curvature).

(2.19)). All the other terms, on both sides of the equations, arise also in steady flow (see Pedley 1980, chapter 4).

The main object of the paper, in both §3 and §4, is to calculate the contributions of the new terms in the equations to the wall shear stress, i.e.

$$\left. \begin{aligned} \text{axial wall shear stress} &= -\hat{w}_{\hat{r}}|_{\hat{r}=a}, \\ \text{azimuthal wall shear stress} &= -\hat{v}_{\hat{r}}|_{\hat{r}=a}. \end{aligned} \right\} \quad (2.26)$$

3. Flow in a tube with uniform, time-dependent curvature

3.1. Formulation

In this section we consider the special case of a curve of uniform curvature which varies with time. We postulate that one cross-section, at $s = 0$, is fixed, with its centre at the origin and the centreline locally in the \hat{y} -direction (figure 3).

Then the equation of the centreline is

$$\hat{y}_0 = af(\hat{s}, \hat{t}) = \frac{a}{\delta(t)} \sin(s\delta(t)), \quad (3.1)$$

where the radius of curvature of the tube is $a\delta(t)^{-1}$, and $s = \hat{s}/a$, $t = \hat{t}/T$ are the dimensionless arclength and time respectively (T is the time scale for the curvature variation). We non-dimensionalize the governing equations (2.22)–(2.25), first by scaling all lengths with a , all velocities with a scale U_0 and pressure with ρU_0^2 . With

f given by (3.1), and noticing that the other functions appearing are

$$C_1 = \sin s\delta, \quad I = \delta^{-1}(1 - \cos s\delta), \quad h = 1 + \delta(t)r \cos \theta, \quad (3.2)$$

we obtain the following equations:

continuity:

$$u_r + \frac{1}{r}v_\theta + \frac{1}{h}w_s + \frac{1}{r}u + \frac{\delta \cos \theta}{h}u - \frac{\delta \sin \theta}{h}v + \frac{Str \cos \theta \dot{\delta}}{h} = 0, \quad (3.3)$$

e_r :

$$\begin{aligned} & Stu_t + uu_r + \frac{1}{r}vu_\theta + \frac{1}{h}wu_s - \frac{1}{r}v^2 \\ & + St^2 \cos \theta \left(-\frac{\ddot{\delta}}{\delta^2} + \frac{2\dot{\delta}^2}{\delta^3} \right) (1 - \cos s\delta) - Sts\dot{\delta} \cos \theta \left(2w + \frac{Stsh\dot{\delta}}{\delta} \right) - \frac{\delta \cos \theta}{h}w^2 \\ & = -p_r - \frac{1}{rhRe} \left(\frac{\partial}{\partial \theta} \left(\frac{h}{r}(v + rv_r - u_\theta) \right) - \frac{\partial}{\partial s} \left(\frac{r}{h}(-\delta \cos \theta w - hw_r + u_s) \right) \right) \\ & - \frac{2St \cos \theta \dot{\delta}}{Reh}, \end{aligned} \quad (3.4)$$

e_θ :

$$\begin{aligned} & Stv_t + uv_r + \frac{1}{r}vv_\theta + \frac{1}{h}wv_s + \frac{1}{r}uv \\ & - St^2 \sin \theta \left(-\frac{\ddot{\delta}}{\delta^2} + \frac{2\dot{\delta}^2}{\delta^3} \right) (1 - \cos s\delta) + Sts\dot{\delta} \sin \theta \left(2w + \frac{Stsh\dot{\delta}}{\delta} \right) + \frac{\delta \sin \theta}{h}w^2 \\ & = -\frac{1}{r}p_\theta + \frac{1}{hRe} \left(\frac{\partial}{\partial r} \left(\frac{h}{r}(v + rv_r - u_\theta) \right) - \frac{\partial}{\partial s} \left(\frac{1}{rh}(-\delta r \sin \theta w + hw_\theta - rv_s) \right) \right) \\ & + \frac{2St \sin \theta \dot{\delta}}{Reh}, \end{aligned} \quad (3.5)$$

e_s :

$$\begin{aligned} & Stw_t + uw_r + \frac{1}{r}vw_\theta + \frac{1}{h}ww_s + St^2 \left(-\frac{\ddot{\delta}}{\delta^2} + \frac{2\dot{\delta}^2}{\delta^3} \right) \sin s\delta \\ & + 2Stus\dot{\delta} \cos \theta - 2Stvs\dot{\delta} \sin \theta - \frac{2St^2s\dot{\delta}^2}{\delta^2} + \frac{St^2s\ddot{\delta}h}{\delta} \\ & + \frac{\delta \cos \theta}{h}uw - \frac{\delta \sin \theta}{h}vw + \frac{St\dot{\delta}r \cos \theta}{h}w \\ & = -\frac{1}{h}p_s + \frac{1}{rRe} \left(\frac{\partial}{\partial \theta} \left(\frac{1}{hr}(hw_\theta - \delta r \sin \theta w - rv_s) \right) \right. \\ & \left. - \frac{\partial}{\partial r} \left(\frac{r}{h}(-hw_r - \delta \cos \theta w + u_s) \right) \right). \end{aligned} \quad (3.6)$$

Here St is the Strouhal number and Re is the Reynolds number, defined by

$$St = \frac{a}{TU_0}, \quad Re = \frac{U_0 a}{\nu}. \quad (3.7)$$

As expected the equations reduce to the time-independent case (see Pedley 1980, equations (4.1)–(4.4)) when $\dot{\delta} = 0$.

We proceed to solve the above equations in the simplest limit only, in which the

curvature is small and varies relatively slowly ($St \ll 1$) with a small amplitude: $\delta = \delta_0(1 + \epsilon \sin t)$ where $\delta_0 \ll 1$, $\epsilon \ll 1$. A steady mean pressure gradient is assumed, i.e. we put

$$-\hat{p}_s = \hat{G} - \hat{p}'_s, \quad (3.8)$$

and thus if \hat{G} is non-dimensionalized with respect to $\rho U_0^2/a$ then

$$-p_s = G - p'_s(r, \theta, s, t). \quad (3.9)$$

We define the Dean number as

$$D = Re^2 G (2\delta_0)^{1/2}. \quad (3.10)$$

D is taken to be $O(1)$ as $\delta_0 \rightarrow 0$, and U_0 (in Re) is taken to be the peak velocity in steady Poiseuille flow in a straight tube, driven by the same mean pressure gradient. Thus we seek the first non-quasi-steady effects on Dean's steady solution, up to the first contribution to steady streaming.

3.2. Solution

As in the steady case, it is convenient to rescale the axial velocity and the coordinates so that the centrifugal force terms are the same order of magnitude as the viscous and inertial terms: $w \rightarrow w(2\delta_0)^{-1/2}$, $s \rightarrow s(2\delta_0)^{-1/2}$.

Further, the Strouhal number, St , is scaled via

$$St \rightarrow (2\delta_0)^{1/2} St$$

and a small-parameter expansion is then carried out in powers of $(2\delta_0)^{1/2}$:

$$\left. \begin{aligned} w &= w_0 + (2\delta_0)^{1/2} w_1 + (2\delta_0) w_2 + \dots, \\ u &= u_0 + (2\delta_0)^{1/2} u_1 + (2\delta_0) u_2 + \dots, \\ v &= v_0 + (2\delta_0)^{1/2} v_1 + (2\delta_0) v_2 + \dots, \\ p &= p_0 + (2\delta_0)^{1/2} p_1 + (2\delta_0) p_2 + \dots \end{aligned} \right\} \quad (3.11)$$

The boundary conditions are $u = v = w = 0$ at $r = 1$.

At $O((2\delta_0)^0)$, (3.3)–(3.6) become continuity:

$$u_{0r} + \frac{1}{r} v_{0\theta} + w_{0s} + \frac{1}{r} u_0 = 0, \quad (3.12)$$

e_r :

$$\begin{aligned} u_0 u_{0r} + \frac{1}{r} v_0 u_{0\theta} + w_0 u_{0s} - \frac{1}{r} v_0^2 - \frac{(1 + \epsilon \sin t)}{2} \cos \theta w_0^2 \\ = -p_{0r} - \frac{1}{r Re} \left(\frac{\partial}{\partial \theta} \left(\frac{1}{r} (v_0 + r v_{0r} - u_{0\theta}) \right) + \frac{\partial}{\partial s} (r w_{0r}) \right), \end{aligned} \quad (3.13)$$

e_θ :

$$\begin{aligned} u_0 v_{0r} + \frac{1}{r} v_0 v_{0\theta} + w_0 v_{0s} + \frac{1}{r} u_0 v_0 + \frac{(1 + \epsilon \sin t)}{2} \sin \theta w_0^2 \\ = -\frac{1}{r} p_{0\theta} + \frac{1}{Re} \left(\frac{\partial}{\partial r} \left(\frac{1}{r} (v_0 + r v_{0r} - u_{0\theta}) \right) - \frac{\partial}{\partial s} \left(\frac{w_{0\theta}}{r} \right) \right), \end{aligned} \quad (3.14)$$

e_s :

$$u_0 w_{0r} + \frac{1}{r} v_0 w_{0\theta} + w_0 w_{0s} = \frac{D}{Re^2} + \frac{1}{r Re} \left(\frac{\partial}{\partial \theta} \left(\frac{1}{r} (w_{0\theta}) \right) - \frac{\partial}{\partial r} (-r w_{0r}) \right). \quad (3.15)$$

At this order the equations are the same as Dean's, apart from the factor $(1 + \epsilon \sin t)$, and the flow is therefore quasi-steady. The axial velocity w_0 is independent of s and the transverse velocities u_0 and v_0 can be derived from a streamfunction ψ_0 :

$$u_0 = \frac{1}{r}\psi_{0\theta}, \quad v_0 = -\psi_{0r}.$$

The Dean solution is obtained in powers of D and is as follows:

$$\begin{aligned} w_0 &= \sum_{n=0}^{\infty} D^{2n+1} w_{0n} \\ &= \frac{1}{4} \frac{D}{Re} (1 - r^2) + \frac{1}{45 \times 8^3} \frac{D^3}{Re} \cos \theta r (1 - r^2) (19 - 21r^2 + 9r^4 - r^6) (1 + \epsilon \sin t) \\ &\quad + O\left(\frac{D^5}{Re}\right), \end{aligned} \tag{3.16}$$

$$\psi_0 = \sum_{n=1}^{\infty} D^{2n} \psi_{0n} = \frac{2}{9 \times 8^3} \frac{D^2}{Re} \sin \theta r \left(1 - \frac{1}{4} r^2\right) (1 - r^2)^2 (1 + \epsilon \sin t) + O\left(\frac{D^4}{Re}\right). \tag{3.17}$$

The $O((2\delta_0)^{1/2})$ equations are continuity:

$$u_{1r} + \frac{1}{r} v_{1\theta} + w_{1s} + \frac{1}{r} u_1 = 0, \tag{3.18}$$

e_r :

$$\begin{aligned} &Stu_{0t} + u_0 u_{1r} + u_1 u_{0r} + \frac{1}{r} v_1 u_{0\theta} + \frac{1}{r} v_0 u_{1\theta} + w_1 u_{0s} + w_0 u_{1s} \\ &\quad - Sts\epsilon \cos t \cos \theta w_0 - \frac{1}{r} 2v_0 v_1 - (1 + \epsilon \sin t) \cos \theta w_0 w_1 \\ &= -p_{1r} + \frac{1}{r Re} \left(\frac{\partial}{\partial \theta} \left(\frac{1}{r} (v_1 + r v_{1r} - u_{1\theta}) \right) + \frac{\partial}{\partial s} (r w_{1r}) \right), \end{aligned} \tag{3.19}$$

e_θ :

$$\begin{aligned} &Stv_{0t} + u_1 v_{0r} + u_0 v_{1r} + \frac{1}{r} v_1 v_{0\theta} + \frac{1}{r} v_0 v_{1\theta} + w_0 v_{1s} + w_1 v_{0s} \\ &\quad + Sts\epsilon \cos t \sin \theta w_0 + \frac{1}{r} u_0 v_1 + \frac{1}{r} u_1 v_0 + (1 + \epsilon \sin t) \sin \theta w_0 w_1 \\ &= -\frac{1}{r} p_{1\theta} - \frac{1}{Re} \left(\frac{\partial}{\partial r} \left(\frac{1}{r} (v_1 + r v_{1r} - u_{1\theta}) \right) - \frac{\partial}{\partial s} \left(\frac{w_{1\theta}}{r} \right) \right), \end{aligned} \tag{3.20}$$

e_s :

$$\begin{aligned} &Stw_{0t} + u_1 w_{0r} + u_0 w_{1r} + \frac{1}{r} v_1 w_{0\theta} + \frac{1}{r} v_0 w_{1\theta} + w_1 w_{0s} + w_0 w_{1s} \\ &= \frac{1}{r Re} \left(\frac{\partial}{\partial \theta} \left(\frac{1}{r} (w_{1\theta}) \right) - \frac{\partial}{\partial r} (-r w_{1r}) \right). \end{aligned} \tag{3.21}$$

The solution is again sought as a power series in D , of the form

$$w_1 = \sum_{n=1}^{\infty} D^n w_{1n}, \quad u_1 = \sum_{n=1}^{\infty} D^n u_{1n}, \quad v_1 = \sum_{n=1}^{\infty} D^n v_{1n}. \tag{3.22}$$

and this leads to a sequence of simple linear problems.

At $O(D)$

$$u_{11r} + \frac{1}{r}v_{11\theta} + w_{11s} + \frac{1}{r}u_{11} = 0, \quad (3.23)$$

$$-Stw_{00} \cos \theta s \epsilon \cos t = -p_{11r} - \frac{1}{rRe} \left(\frac{\partial}{\partial \theta} \left(\frac{1}{r}(v_{11} + rv_{11r} - u_{11\theta}) \right) - \frac{\partial}{\partial s} (-rw_{11r}) \right), \quad (3.24)$$

$$Stw_{00} \sin \theta s \epsilon \cos t = -\frac{1}{r}p_{11\theta} + \frac{1}{Re} \left(\frac{\partial}{\partial r} \left(\frac{1}{r}(v_{11} + rv_{11r} - u_{11\theta}) \right) - \frac{\partial}{\partial s} \left(\frac{1}{r}w_{11\theta} \right) \right), \quad (3.25)$$

$$Stw_{00t} = \frac{1}{rRe} \nabla^2 w_{11}. \quad (3.26)$$

Since $w_{00t} = 0$ and $w_{11} = 0$ at $r = 1$ it follows that w_{11} is identically zero and so, from the continuity equation, u_{11} and v_{11} can be written in terms of a streamfunction ψ_{11} . By eliminating p_{11} from the \hat{r} and $\hat{\theta}$ equations, ψ_{11} is found to be

$$\psi_{11} = \frac{1}{384} St \epsilon s \cos t \sin \theta r(1 - r^2)^2. \quad (3.27)$$

The $O(D^2)$ equations are

$$u_{12r} + \frac{1}{r}v_{12\theta} + w_{12s} + \frac{1}{r}u_{12} = 0, \quad (3.28)$$

$$Stu_{00t} + w_{00}u_{11s} = -p_{12r} - \frac{1}{rRe} \left(\frac{\partial}{\partial \theta} \left(\frac{1}{r}(v_{12} + rv_{12r} - u_{12\theta}) \right) + \frac{\partial}{\partial s} (rw_{12r}) \right), \quad (3.29)$$

$$Stv_{00t} + w_{00}v_{11s} = -\frac{1}{r}p_{12\theta} + \frac{1}{Re} \left(\frac{\partial}{\partial r} \left(\frac{1}{r}(v_{12} + rv_{12r} - u_{12\theta}) \right) - \frac{\partial}{\partial s} \left(\frac{1}{r}w_{12\theta} \right) \right), \quad (3.30)$$

$$u_{11}w_{00r} = \frac{1}{Re} \nabla^2 w_{12}. \quad (3.31)$$

From the axial equation w_{12} is found to be

$$w_{12} = -\frac{1}{36864} St \epsilon s \cos t \cos \theta (-3r + 6r^3 - 4r^5 + r^7) \quad (3.32)$$

and u_{12} and v_{12} are found to be proportional to $s \cos t$.

At $O(2\delta_0)$ we again seek solutions for w_2, u_2, v_2 in powers of D , in the form

$$w_2 = \sum_{n=1}^{\infty} D^n w_{2n}, \quad u_2 = \sum_{n=1}^{\infty} D^n u_{2n}, \quad v_2 = \sum_{n=1}^{\infty} D^n v_{2n}, \quad (3.33)$$

and the $O(D)$ equations are

$$u_{21r} + \frac{1}{r}v_{21\theta} + w_{21s} + \frac{1}{r}u_{21} = 0, \quad (3.34)$$

$$Stu_{11t} = -p_{21r} - \frac{1}{rRe} \left(\frac{\partial}{\partial \theta} \left(\frac{1}{r}(v_{21} + rv_{21r} - u_{21\theta}) \right) + \frac{\partial}{\partial s} (rw_{21r}) \right), \quad (3.35)$$

$$Stv_{11t} = -\frac{1}{r}p_{21\theta} + \frac{1}{Re} \left(\frac{\partial}{\partial r} \left(\frac{1}{r}(v_{21} + rv_{21r} - u_{21\theta}) \right) - \frac{\partial}{\partial s} \left(\frac{1}{r}w_{21\theta} \right) \right), \quad (3.36)$$

$$0 = -\frac{(1 + \epsilon \sin t)r \cos \theta}{2Re^2} - p_{01s} + \frac{1}{Re} \nabla^2 w_{21} + \frac{1}{rRe} \left(\frac{\partial}{\partial \theta} \left(-\frac{\sin \theta(1 + \epsilon \sin t)}{2} w_0 \right) - \frac{\partial}{\partial r} \left(\frac{-r \cos \theta(1 + \epsilon \sin t)}{2} w_0 \right) \right). \quad (3.37)$$

From the axial equation w_{21} is given by

$$w_{21} = \frac{3}{32Re} (1 + \epsilon \sin t) \cos \theta (r^3 - r)$$

which is proportional to the basic quasi-steady Dean solution again. Since w_{21} is independent of s there exists a streamfunction ψ_{21} and it can be seen that this is proportional to $s \sin t$. In fact we find that ψ_{21} is

$$\psi_{21} = -\frac{1}{18432} St^2 Re \epsilon s \sin t \sin \theta (r^7 - 4r^5 + 5r^3 - 2r), \quad (3.38)$$

and also that p_{21} is given as

$$p_{21} = \frac{1}{2304} St^2 \epsilon sr \sin t \cos \theta. \quad (3.39)$$

At $O(D^2)$ the flow separates into mean and time-dependent parts. The equations are

$$u_{22r} + \frac{1}{r} v_{22\theta} + w_{22s} + \frac{1}{r} u_{22} + \frac{1}{2} (1 + \epsilon \sin t) u_{01} - \frac{1}{2} (1 + \epsilon \sin t) v_{01} = 0, \quad (3.40)$$

$$\begin{aligned} &Stu_{12t} + u_{11}u_{11r} + \frac{1}{r}v_{11}u_{11\theta} + w_{11}u_{11s} + w_{00}u_{21s} - \frac{1}{r}v_{11}v_{11} \\ &- Sts\epsilon \cos t \cos \theta w_{12} - (1 + \epsilon \sin t) \cos \theta w_{00}w_{21} + \frac{1}{4}(1 + \epsilon \sin t)^2 r \cos \theta w_{00}^2 \\ &= -p_{22r} + [s\text{-indep. terms}] - \frac{1}{rRe} \left(\frac{\partial}{\partial \theta} \left(\frac{1}{r} (v_{22} + rv_{22r} - u_{22\theta}) \right) - \frac{\partial}{\partial s} (-rw_{22r}) \right), \end{aligned} \quad (3.41)$$

$$\begin{aligned} &Stv_{12t} + u_{11}v_{11r} + \frac{1}{r}v_{11}v_{11\theta} + w_{11}v_{11s} + w_{00}v_{21s} + \frac{1}{r}u_{11}v_{11} \\ &+ Sts\epsilon \cos t \sin \theta w_{12} + (1 + \epsilon \sin t) \sin \theta w_{00}w_{21} - \frac{1}{4}(1 + \epsilon \sin t)^2 r \cos \theta \sin \theta w_{00}^2 \\ &= -\frac{1}{r}p_{22\theta} + [s\text{-indep. terms}] + \frac{1}{Re} \left(\frac{\partial}{\partial r} \left(\frac{1}{r} (v_{22} + rv_{22r} - u_{22\theta}) \right) - \frac{\partial}{\partial s} \left(\frac{1}{r} w_{22\theta} \right) \right), \end{aligned} \quad (3.42)$$

$$Stw_{12t} + u_{21}w_{00r} + w_{00}w_{21s} = \frac{1}{Re} \nabla^2 w_{22} - p_{02s}. \quad (3.43)$$

From the radial and circumferential equations of motion the mean secondary streamfunction, ψ_{22}^s and the mean pressure, p_{22}^s , can be found and are given by

$$\psi_{22}^s = -\frac{1}{147557760} \sin(2\theta) s^2 \epsilon^2 Re St^2 (r^{10} - 20r^6 + 36r^4 - 17r^2). \quad (3.44)$$

The pressure is found to be

$$\begin{aligned} p_{22}^s = \frac{1}{2} \left(\frac{1}{1474560} \cos(2\theta) Re St^2 \epsilon^2 s^2 (41r^2 - \frac{220}{3}r^4 + 60r^6 - 18r^8) \right. \\ \left. + \frac{1}{196608} Re St^2 \epsilon^2 s^2 \left(\frac{1}{4}r^2 - \frac{4}{3}r^4 - \frac{16}{9}r^6 + r^8 \right) \right). \end{aligned} \quad (3.45)$$

It should be noted that these are the non-quasi-steady contributions to the streamfunction and pressure and are dependent upon s^2 .

Finally, the $O(D^3)$ axial equation is

$$\begin{aligned} & Stw_{12t} + u_{22}w_{00r} + u_{11}w_{12r} + u_{01}w_{21r} + \frac{1}{r}(v_{11}w_{12\theta} + v_{01}w_{21\theta}) \\ & + \frac{\cos\theta(1 + \epsilon \sin t)}{2}u_{01}w_{00} - \frac{(1 + \epsilon \sin t)\sin\theta}{2}v_{01}w_{00} \\ & = -p_{03s} + \frac{1}{Re}\nabla^2 w_{23} \\ & + \frac{1}{rRe}\left(\frac{\partial}{\partial\theta}\left(\frac{\sin\theta}{2}w_{03}(1 + \epsilon \sin t)\right) - \frac{\partial}{\partial r}\left(-\frac{r\cos\theta}{2}w_{03}(1 + \epsilon \sin t)\right)\right) \end{aligned} \quad (3.46)$$

and from this equation it is found that the mean axial velocity is given by

$$\begin{aligned} w_{23} = & St^2 Re \epsilon^2 s^2 \left(\frac{1}{237817036800}(r^2 - 2380r^4 + 2415r^6 - 1260r^8 \right. \\ & \left. + 350r^{10} - 48r^{12})\right) \cos(2\theta) \\ & + St^2 Re \epsilon^2 s^2 \left(\frac{1}{6794772480}(-37 + 180r^2 - 360r^4 + 380r^6 \right. \\ & \left. - 225r^8 + 72r^{10} - 10r^{12})\right). \end{aligned} \quad (3.47)$$

The mean terms in ψ_{22} and w_{23} represent the first effect of the time-dependence on the mean flow, and are therefore the leading terms in the steady streaming.

In summary, the axial velocity is given by

$$\begin{aligned} w = & \frac{D}{4Re}(1 - r^2) \\ & + \frac{1}{45 \times 8^3} \frac{D^3}{Re} \cos\theta r(1 - r^2)(19 - 21r^2 + 9r^4 - r^6)(1 + \epsilon \sin t) + O\left(\frac{D^5}{Re}\right) \\ & + (2\delta_0)^{1/2} \left(D^2(-St\epsilon s \cos t \cos\theta \frac{1}{36864}(-3r + 6r^3 - 4r^5 + r^7)) + O(D^3)\right) \\ & + (2\delta_0) \left(\frac{3}{32} \frac{D}{Re}(1 + \epsilon \sin t) \cos\theta(r^3 - r) + (D^2 Re)\text{time-dependent terms}\right) \\ & + (D^3(St^2 Re \epsilon^2 s^2 \left(\frac{1}{237817036800}(923r^2 - 2380r^4 + 2415r^6 - 1260r^8 \right. \\ & \left. + 350r^{10} - 48r^{12})\right) \cos(2\theta) \\ & + St^2 Re \epsilon^2 s^2 \left(\frac{1}{6794772480}(-37 + 180r^2 - 360r^4 + 380r^6 - 225r^8 + 72r^{10} - 10r^{12})\right) \\ & + \text{time-dependent terms}) + O(D^4 Re) + O((2\delta_0)^{3/2}). \end{aligned} \quad (3.48)$$

The secondary streamfunction is given by

$$\begin{aligned} \psi = & \frac{2}{9 \times 8^3} \frac{D^2}{Re} r(1 - \frac{1}{4}r^2)(1 - r^2)^2(1 + \epsilon \sin t) \sin\theta + O\left(\frac{D^4}{Re}\right) \\ & + (2\delta_0)^{1/2} (DSt\epsilon s \cos t \sin\theta \frac{1}{384}(r^5 - 2r^3 + r) + O(D^2)) \\ & + (2\delta_0)(D(-St^2 Re \epsilon s \sin t \sin\theta \frac{1}{18432}(r^7 - 4r^5 + 5r^3 - 2r) \\ & + D^2(-\frac{1}{141557760}s^2 \epsilon^2 Re St^2 \sin(2\theta)(r^{10} - 20r^6 - 17r^2 + 36r^4)) + O(D^3 Re) \\ & + O((2\delta_0)^{3/2})). \end{aligned} \quad (3.49)$$

The quantity of greatest interest is the wall shear stress (WSS, equations (2.26)) which can be split up into axial and azimuthal components. The leading contributions to

the mean and time-dependent parts of each are as follows:

$$\begin{aligned} \text{Mean axial WSS:} &= \frac{1}{2} \frac{D}{Re} + \frac{6}{45 \times 8^5} \frac{D^3}{Re} \cos \theta + O\left(\frac{D^5}{Re}\right) \\ &+ (2\delta_0) \left(\frac{17}{11890851840} D^3 Re St^2 s^2 \epsilon^2 \cos(2\theta) + O(D^4 Re)\right), \end{aligned} \quad (3.50)$$

$$\begin{aligned} \text{Time-dependent axial WSS:} &= \frac{6}{45 \times 8^5} \frac{D^3}{Re} \epsilon \cos \theta \sin t + O\left(\frac{D^5}{Re}\right) \\ &+ (2\delta_0)^{1/2} \left(\frac{1}{18432} D^2 St s \epsilon \cos t \cos \theta + O(D^3)\right), \end{aligned} \quad (3.51)$$

$$\begin{aligned} \text{Mean azimuthal WSS:} &= \frac{1}{6 \times 8^2} \frac{D^2}{Re} \sin \theta + O\left(\frac{D^4}{Re}\right) \\ &+ (2\delta_0) \left(\frac{7}{8847360} D^2 Re St^2 s^2 \epsilon^2 \sin(2\theta) + O(D^3 Re)\right), \end{aligned} \quad (3.52)$$

$$\begin{aligned} \text{Time dependent azimuthal WSS:} &= \frac{1}{6 \times 8^2} \frac{D^2}{Re} \epsilon \sin \theta \sin t + O\left(\frac{D^4}{Re}\right) \\ &+ (2\delta_0)^{1/2} \left(\frac{1}{48} D St s \epsilon \cos t \sin \theta + O(D^2)\right). \end{aligned} \quad (3.53)$$

3.3. Discussion

The above analysis has calculated the principal corrections introduced by the time-dependence of curvature to the axial and secondary flows found by Dean (1927,1928), with particular reference to the wall shear stress.

As discussed in §2 the introduction of time-dependent curvature into the system has led us to choose a non-inertial frame of reference. With respect to this frame of reference the position of the centreline of the tube is fixed. However with respect to an inertial frame of reference the motion of this centreline (and indeed the pipe) may be thought of as consisting of two parts: a rotational part that gives rise to ‘Coriolis’ and ‘centrifugal’ forces and a translational part. It can be shown that the centrifugal effects due to the rotation of the pipe and the translational effects due to the movement of the centreline can be absorbed into a reduced pressure.

At $O((\delta_0)^0)$ the flow is quasi-steady Dean-type flow. There is a correction to straight-tube Poiseuille flow due to the centrifugal effect of flow along a curved path, and there is a secondary motion directed towards the outside of the bend in the centre of the tube, and back towards the inside near the walls.

At $O((2\delta_0)^{1/2})$ a further secondary streamfunction $D\psi_{11}$ is derived from the Coriolis terms. This secondary streaming is also directed towards the outside of the bend in the centre of the tube for $\cos t > 0$, when the rotation is in the positive sense, and towards the inside of the bend for $\cos t < 0$, when the rotation is in the negative sense. Thus for $0 < t < \frac{1}{2}\pi$ and $\frac{3}{2}\pi < t < 2\pi$ faster-moving fluid is moved more towards the outside of the bend than in Dean flow while for $\frac{1}{2}\pi < t < \frac{3}{2}\pi$ faster-moving fluid is moved more towards the inside of the bend. This is represented by the term w_{12} and results in an increase in axial wall shear stress on the outside of the bend for $\cos t > 0$ and on the inside of the bend for $\cos t < 0$. The same effect arises in a rotating pipe of fixed (e.g. zero) curvature and is solely due to the rotation. We note that the contribution to azimuthal wall shear stress is $O((2\delta_0)^{1/2} D St \epsilon s)$ compared with $O(D^2/Re)$ for Dean flow. Dimensionally, therefore, the Dean azimuthal wall shear stress is $O((2\delta_0)\hat{G}^2 a^4/\rho^2 v^3)$ and the new contribution is $O((2\delta_0)\hat{G}\epsilon\hat{s}a^2/\rho v^2 T)$.

Similarly, we see that the contribution to axial wall shear stress is $O((2\delta_0)^{1/2}D^2Stes)$ compared with $O(D/Re)$ for Poiseuille flow and $O(D^3/Re)$ for the first Dean correction to Poiseuille flow. Dimensionally the first Dean correction to axial wall shear stress is $O((2\delta_0)G^3a^6/v^5\rho^3)$ while the new contribution is $O((2\delta_0)G^2\epsilon\hat{s}a^5/v^4\rho^2T)$.

At $O((2\delta_0)^1)$ a time-dependent streamfunction, ψ_{21} , is found that is out of phase with ψ_{11} . In the first quarter of the cycle, when the rotation is in the positive sense, ψ_{21} is in the same direction as ψ_{11} but is increasing in magnitude while ψ_{11} is decreasing. In the next quarter-cycle, corresponding to negative rotation, ψ_{21} retains its direction, despite the change in rotational direction, but decreases in magnitude as it adjusts to the change in the direction of rotation, while ψ_{11} has reversed its direction, corresponding to the change in rotation direction, and increases in magnitude. In the next quarter, ψ_{21} reverses direction, so that it is now in the same sense as ψ_{11} , and increases in magnitude while ψ_{11} maintains its direction but decreases in magnitude. Finally in the latter quarter of the cycle, ψ_{11} once again changes direction and increases in strength while ψ_{21} maintains its direction, in the opposite sense to the rotation, but again decreases in magnitude. Thus ψ_{11} is the irrotational response of the fluid due to the rotation of the tube while ψ_{21} represents a delay or 'lag' in the fluid response, accounting for the inertia of the fluid. ψ_{11} changes sense as the rotation changes direction while ψ_{21} 'lags' behind with a phase shift of $\frac{1}{2}\pi$ (see figure 4).

Also at this order there is a steady secondary streaming that is derived from the convective inertia terms and also from the Coriolis term $-Stes \cos t \cos \theta w_{12}$. At this order Dw_{12} is a Dean-type correction to the axial velocity while D^2w_{22} is a time-dependent axial velocity correction, driven by the time-dependent secondary streamfunction ψ_{21} . It results in an increase in axial wall shear stress on the outside wall for the first half of the cycle and a decrease in axial wall shear stress on the outside wall for the second half of the cycle. w_{23} is the mean part of the axial velocity that is generated by the inertial convection of the Poiseuille flow due to the mean secondary streaming and the inertial convection of the primary correction to the axial flow by the primary correction to the secondary streamfunction.

The first effect that arises due to the curvature being time-dependent originates from the $St^2(-\ddot{\delta}/\delta^2 + 2\dot{\delta}/\delta^3)\sin s\delta$ term in (3.6); this comes from the terms representing the acceleration of the frame of reference, involving $f_{\hat{t}\hat{t}}, I_{\hat{t}\hat{t}}, \hat{r}f_{\hat{s}\hat{t}\hat{t}}$. The first power in the $\sin s\delta$ series cancels with the other terms involving $f_{\hat{t}\hat{t}}, I_{\hat{t}\hat{t}}, \hat{r}f_{\hat{s}\hat{t}\hat{t}}$ and so the first effect is order $St^2(-\ddot{\delta}/\delta^2 + 2\dot{\delta}/\delta^3)(-s^3\delta^3/3!)$ which, after scaling, gives rise to an axial velocity term of order $(2\delta_0)^2$. This gives a wall shear stress at a higher order in $(2\delta_0)^{1/2}$ than has so far been calculated. Since all the calculated flow components depend algebraically upon s , the above effects become more pronounced as one moves farther from the origin. The solution will no longer be valid for $|s| = O(\delta_0^{-1/2})$, i.e. dimensional distance $O(a\delta_0^{-1/2})$.

The streamfunction is now

$$\psi = \frac{2 \sin \theta D^2}{9 \times 8^3 Re} r \left(1 - \frac{1}{4}r^2\right) (1 - r^2)^2 (1 + \epsilon \sin t) + (2\delta_0)^{1/2} \left(\frac{DStes \cos t \sin \theta}{384} (r^5 - 2r^3 + r) \right). \quad (3.54)$$

A secondary stagnation point occurs where $\theta = \frac{1}{2}\pi$ and $\psi_r = 0$. Dean found the stagnation point to be at $r = r_0 \approx 0.43$. To find the correction due to varying

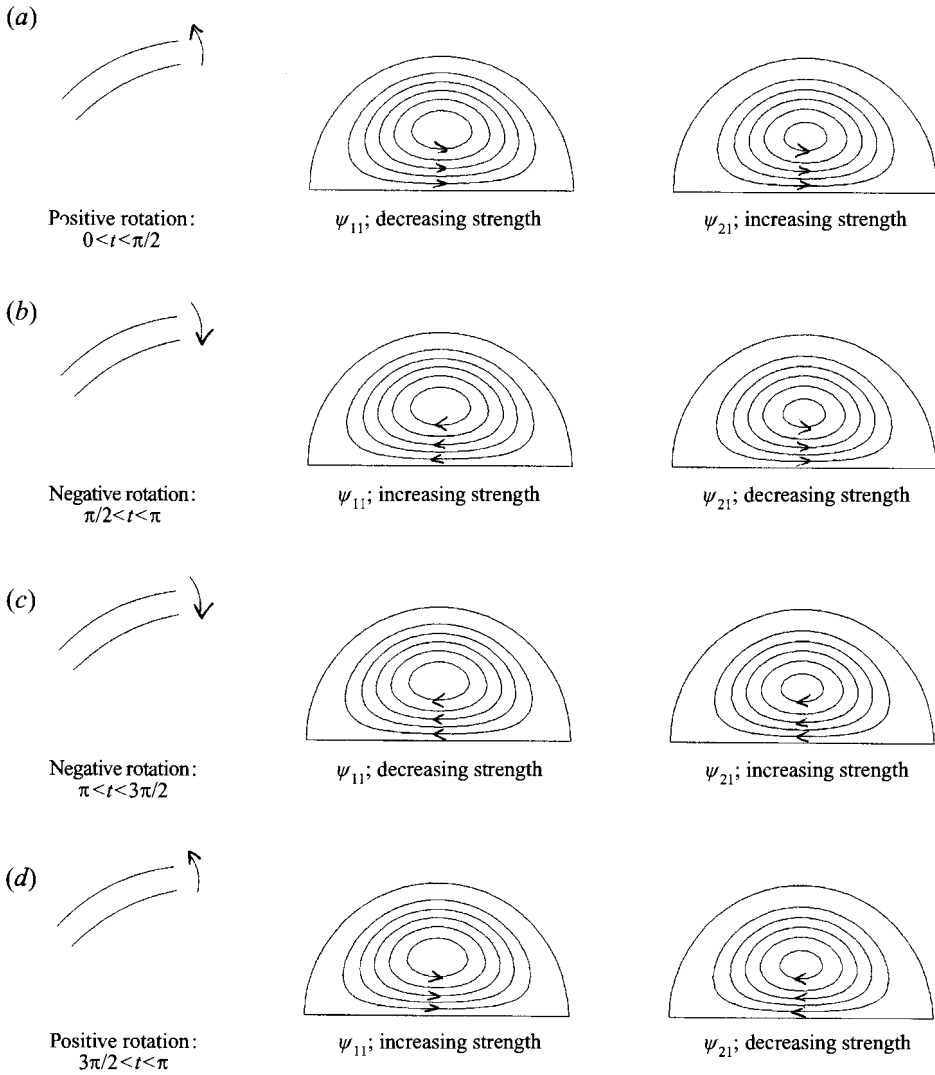


FIGURE 4. The directions and strengths of the first two corrections to the Dean secondary streamfunction: (a) $0 < t < \pi/2$, rotation in the positive sense; (b) $\pi/2 < t < \pi$, rotation in the negative sense; (c) $\pi < t < 3\pi/2$, rotation in the negative sense; (d) $3\pi/2 < t < 2\pi$, rotation in the positive sense.

curvature, we take $r = r_0 + r'$, where $|r'| \ll r_0$, and obtain

$$r' \approx 0.1(2\delta_0)^{1/2} ReSt\epsilon \cos t D^{-1} + O(2\delta_0).$$

Thus the secondary stagnation point is moved outwards when $\cos t$ is positive and inwards when $\cos t$ is negative.

4. Flow in a time-dependent sinuous tube

4.1. Formulation

In this section we consider the flow through a pipe of circular cross-section, radius a , whose time-dependent shape is a small oscillatory perturbation from a straight pipe.

Steady and pulsatile flow through fixed sinusoidal tubes of very small amplitude have been studied by Murata, Miyake & Inaba (1976) and by Inaba & Murata (1978). We here suppose that somewhere upstream the straight pipe is undisturbed. The variables $\hat{r}, \hat{s}, \hat{t}, \hat{u}, \hat{v}, \hat{w}, \hat{p}$ are again non-dimensionalized with respect to $a, a, T, U_0, U_0, U_0, \rho U_0^2$, where U_0 is the mean axial velocity upstream and T is the period of the imposed oscillation. We consider the centreline to be defined by

$$f(\hat{s}, \hat{t}) = \epsilon b g(s, t) \quad (4.1)$$

where it is assumed that $\epsilon \ll 1$ and, initially, $b \sim O(1)$. The non-dimensionalized versions of equations (2.22)–(2.25) are then

$$u_r + \frac{1}{r} v_\theta + h^{-1} w_s + \frac{1}{r} u - \epsilon b C_1^{-1} h^{-1} (g_{ss} [\cos \theta u - \sin \theta v] + St r \cos \theta [g_{sst} + \epsilon^2 b^2 g_s g_{ss} g_{st} C_1^{-2}]) = 0, \quad (4.2)$$

$$\begin{aligned} St u_t + uu_r + \frac{1}{r} v u_\theta + h^{-1} w u_s - \frac{1}{r} v^2 + \epsilon b g_{ss} C_1^{-1} h^{-1} \cos \theta w^2 \\ + 2 St \epsilon b g_{st} C_1^{-1} \cos \theta w + St^2 \epsilon b [g_{tt} C_1 - g_s I_{tt}] \cos \theta - St^2 \epsilon^2 b^2 r g_{st}^2 C_1^{-2} \cos^2 \theta \\ = -p_r + \frac{1}{Re} \left\{ \frac{1}{r^2} u_{\theta\theta} + h^{-2} u_{ss} - \frac{1}{r} v_{r\theta} - \epsilon b g_{ss} C_1^{-1} h^{-1} \sin \theta \left(v_r - \frac{1}{r} u_\theta + \frac{1}{r} v \right) \right. \\ \left. - \frac{1}{r^2} v_\theta - h^{-1} w_{rs} + \epsilon b C_1^{-1} h^{-3} \cos \theta [g_{sss} + \epsilon^2 b^2 g_s g_{ss}^2 C_1^{-2}] [w + r u_s] \right. \\ \left. + \epsilon b g_{ss} C_1^{-1} h^{-2} \cos \theta w_s + 2 St \epsilon b C_1^{-1} h^{-1} \cos \theta [g_{sst} + \epsilon^2 b^2 g_s g_{ss} g_{st} C_1^{-2}] \right\}, \quad (4.3) \end{aligned}$$

$$\begin{aligned} St v_t + w v_r + \frac{1}{r} v v_\theta + h^{-1} w v_s + \frac{1}{r} w v - St^2 \epsilon b [g_{tt} C_1 - g_s I_{tt}] \sin \theta \\ - \epsilon b g_{ss} C_1^{-1} h^{-1} \sin \theta w^2 - 2 St \epsilon b g_{st} C_1^{-1} \sin \theta w + St^2 \epsilon^2 b^2 r g_{st}^2 C_1^{-2} \sin \theta \cos \theta \\ = -\frac{1}{r} p_\theta + \frac{1}{Re} \left\{ v_{rr} + h^{-2} v_{ss} - r^{-1} h^{-1} w_{\theta s} - \frac{1}{r} u_{r\theta} + r^{-2} h^{-1} u_\theta + \frac{1}{r} v_r \right. \\ \left. - r^{-2} h^{-1} v - \epsilon b C_1^{-1} h^{-1} g_{ss} \cos \theta v_r - \epsilon b C_1^{-1} h^{-2} g_{ss} \sin \theta w_s \right. \\ \left. - \epsilon b C_1^{-1} h^{-3} [g_{sss} + \epsilon^2 b^2 g_s g_{ss}^2 C_1^{-2}] [\sin \theta w - r \cos \theta v_s] \right. \\ \left. - 2 St \epsilon b C_1^{-1} h^{-1} \sin \theta [g_{sst} + \epsilon^2 b^2 g_s g_{ss} g_{st} C_1^{-2}] \right\}, \quad (4.4) \end{aligned}$$

$$\begin{aligned} St w_t + u w_r + \frac{1}{r} v w_\theta + h^{-1} w w_s - \epsilon b g_{ss} C_1^{-1} h^{-1} (\cos \theta u - \sin \theta v) w \\ - St \epsilon b r C_1^{-1} h^{-1} \cos \theta [g_{sst} + \epsilon^2 b^2 g_s g_{ss} g_{st} C_1^{-2}] w + St^2 \epsilon^2 b^2 g_s g_{st} + St^2 C_1 I_{tt} \\ - 2 St \epsilon b g_{st} C_1^{-1} (\cos \theta u - \sin \theta v) - St^2 \epsilon b r C_1^{-1} \cos \theta [g_{stt} + \epsilon^2 b^2 g_s g_{st}^2 C_1^{-2}] \\ = -\frac{1}{h} p_s + \frac{1}{Re} \left\{ w_{rr} + \frac{1}{r^2} w_{\theta\theta} - h^{-1} u_{rs} - r^{-1} h^{-2} u_s + \frac{1}{r} w_r - r^{-1} h^{-1} v_{\theta s} \right. \\ \left. + \epsilon b g_{ss} C_1^{-1} h^{-1} \left(h^{-1} \sin \theta v_s + \frac{1}{r} \sin \theta w_\theta - \cos \theta w_r \right) - \epsilon^2 b^2 g_{ss}^2 C_1^{-2} h^{-2} w \right\}, \quad (4.5) \end{aligned}$$

where the Strouhal and Reynolds numbers are again defined by (3.7).

Following Smith (1976*a,b*), we note that because $Re \gg 1$ the core flow is essentially

inviscid and its perturbation from Poiseuille flow only $O(\epsilon)$. Accordingly, the flow field in the core is expanded asymptotically:

$$\left. \begin{aligned} u &= \epsilon u_1(r, \theta, s, t) + O(\epsilon^2), & w &= w_0(r) + \epsilon w_1(r, \theta, s, t) + O(\epsilon^2), \\ v &= \epsilon v_1(r, \theta, s, t) + O(\epsilon^2), & p &= -\frac{S}{Re} + \epsilon p_1(r, \theta, s, t) + O(\epsilon^2), \end{aligned} \right\} \quad (4.6)$$

where Poiseuille flow takes the form $w_0(r) = \frac{1}{4}(1 - r^2)$. We also note that $I_{tt} = O(\epsilon^2 b^2)$, $h = 1 + O(\epsilon b)$, and $C_1 = 1 + O(\epsilon^2 b^2)$. With the assumption that $St \ll 1$ and $Re^{-1} \ll \epsilon$ first-order equations of motion:

$$\left. \begin{aligned} u_{1r} + \frac{1}{r}u_1 + \frac{1}{r}v_{1\theta} + w_{1s} &= 0, & w_0 u_{1s} + b g_{ss} \cos \theta w_0^2 &= -p_{1r}, \\ w_0 v_{1s} - b g_{ss} \sin \theta w_0^2 &= -\frac{1}{r}p_{1\theta}, & u_1 w_{0r} + w_0 w_{1s} &= -p_{1s}. \end{aligned} \right\} \quad (4.7)$$

At this order the core flow is quasi-steady, although it is the time-dependent $b g_{ss} \cos \theta w_0^2$, $b g_{ss} \sin \theta w_0^2$ terms that force a non-trivial solution. The inviscid flow boundary condition is $u_1(1, \theta, s, t) = 0$.

The unique solution that satisfies this condition and matches to the flow in a straight pipe upstream is

$$\left. \begin{aligned} u_1 &= -b w_0 \cos \theta g_s, & v_1 &= b w_0 \sin \theta g_s, \\ w_1 &= b w_{0r} \cos \theta g, & p_1 &= 0. \end{aligned} \right\} \quad (4.8)$$

Transformed back to the inertial frame of reference, this solution shows that, at this order, streamlines in the core carry on in straight lines parallel to the x -axis. The solution is the same as that given by Smith (1976a,b) for pipe flows perturbed by non-axisymmetric wall distortions.

The axial velocity does not satisfy the no-slip boundary condition, $w(1, \theta, s, t) = 0$, (in fact, $w_1 = -\frac{1}{2} \cos \theta g$ at $r = 1$) and hence a (viscous) boundary layer is required. Matching of the terms in the continuity equation and the inertia, pressure and viscous terms in the axial momentum equation requires this layer to be of thickness ϵ which must in turn be $O(Re^{-1/3})$. The time-dependence has a simple but non-trivial effect if, further, $St = O(\epsilon)$. Then the flow field is given by

$$\left. \begin{aligned} u &= -Re^{-2/3} U + O(Re^{-1}), & v &= Re^{-1/3} V + O(Re^{-2/3}), \\ w &= Re^{-1/3} W + O(Re^{-2/3}), & p &= Re^{-2/3} P + O(Re^{-1}), \end{aligned} \right\} \quad (4.9)$$

where $r = 1 - Re^{-1/3} Y$ defines the boundary-layer coordinate Y . This yields the non-quasi-steady boundary-layer equations

$$\left. \begin{aligned} U_Y + V_\theta + W_s &= 0, & P_Y &= 0, \\ V_t + UV_Y + VV_\theta + WW_s &= -P_\theta + V_{YY}, \\ W_t + UW_Y + VW_\theta + WW_s &= -P_s + W_{YY}, \end{aligned} \right\} \quad (4.10)$$

with boundary conditions

$$U = V = W = 0 \quad \text{on} \quad Y = 0 \quad (4.11)$$

and matching conditions with the core flow of

$$V \rightarrow 0, \quad W \rightarrow \frac{1}{2}Y - \frac{1}{2}b \cos \theta g \quad \text{as} \quad Y \rightarrow \infty. \quad (4.12)$$

4.2. Linearized solution

To solve these equations we first linearize with respect to b by assuming $Re^{-1/3} = \epsilon \ll b \ll 1$ so that b is not so small as to interfere with the orders of the equations,

and then remove the θ -dependence with the substitution

$$(U, W - \frac{1}{2}Y, P) = b(U_a, W_a, P_a) \cos \theta, \quad V = bV_a \sin \theta,$$

where U_a, V_a, W_a are functions of Y, s, t and P_a is a function of s, t only. We can now use a Fourier transform approach to solve the equations. Defining

$$W^*(Y, \alpha, \gamma) = \int_{-\infty}^{\infty} \int_{-\infty}^{\infty} W_a(Y, s, t) e^{-i\alpha s} e^{-i\gamma t} ds dt, \quad \text{etc.}, \quad (4.13)$$

we obtain the transformed boundary-layer equations:

$$\left. \begin{aligned} U_Y^* + V^* + i\alpha W^* &= 0, & P_Y^* &= 0, \\ i\gamma V^* + \frac{1}{2}i\alpha Y V^* &= P^* + V_{YY}^*, \\ i\gamma W^* + \frac{1}{2}U^* + \frac{1}{2}i\alpha Y W^* &= -i\alpha P^* + W_{YY}^*, \\ U^* = V^* = W^* &= 0 \text{ on } Y = 0, \\ V^* \rightarrow 0, \quad W^* &\rightarrow -\frac{1}{2}g^* \text{ as } Y \rightarrow \infty. \end{aligned} \right\} \quad (4.14)$$

Eliminating U^* to give

$$i\gamma W_Y^* - \frac{1}{2}V^* + \frac{1}{2}i\alpha Y W_Y^* = W_{YY}^*, \quad (4.15)$$

and introducing a new radial variable $\xi = \Delta^{1/3}Y + \xi_0$, where $\Delta = \frac{1}{2}i\alpha$ and $\xi_0 = i\gamma\Delta^{-2/3}$ reduces equations (4.14), for V^* , and (4.15), for W_Y^* , to inhomogeneous Airy equations. Their solutions (cf. Smith 1976a) satisfying the boundary conditions at $Y = 0$ and ∞ , are

$$V^* = -\Delta^{-2/3}P^*L(\xi) \quad (4.16)$$

and

$$W^* = B^*(\alpha, \gamma) \int_{\xi_0}^{\xi} \text{Ai}(q) dq + \frac{1}{2}\Delta^{-5/3}P^*L(\xi), \quad (4.17)$$

where

$$L(\xi) = \text{Ai}(\xi) \int_{\xi_0}^{\xi} \frac{dq}{\text{Ai}(q)^2} \int_{\infty}^q \text{Ai}(t) dt. \quad (4.18)$$

Here, $\text{Ai}(\xi)$ is the Airy function and $L(\xi_0) = 0, L(\infty) = 0, L_{\xi\xi}(\xi_0) = 1$ so that the wall boundary conditions are satisfied and the azimuthal velocity matches that in the core. The branch chosen for $\Delta^{1/3}$ is that which implies a branch cut along the positive imaginary α -axis.

To find the unknown P^* and B^* , we use the matching condition for the axial velocity, namely

$$B^* \int_{\xi_0}^{\infty} \text{Ai}(q) dq + 0 = -\frac{1}{2}g^*,$$

and set $Y = 0$ (or $\xi = \xi_0$) in the axial equation to give

$$i\alpha P^* = W_{YY}^*|_{Y=0} = \Delta^{2/3} (B^* \text{Ai}'(\xi_0) + \frac{1}{2}\Delta^{-5/3}P^*).$$

Thus,

$$B^* = -\frac{1}{2} \left(\int_{\xi_0}^{\infty} \text{Ai}(q) dq \right)^{-1} g^*, \quad (4.19)$$

$$P^* = \Delta^{5/3} \text{Ai}'(\xi_0) (1 + \alpha^2)^{-1} \left(\int_{\xi_0}^{\infty} \text{Ai}(q) dq \right)^{-1} g^*, \quad (4.20)$$

$$V_Y^*|_{Y=0} = \frac{\Delta^{4/3} \text{Ai}'(\xi_0)}{(1 + \alpha^2) \text{Ai}(\xi_0)} g^*, \tag{4.21}$$

$$W_Y^*|_{Y=0} = -\frac{1}{2} \Delta^{1/3} \frac{\text{Ai}(\xi_0)}{\int_{\xi_0}^{\infty} \text{Ai}(q) dq} \left\{ 1 + \frac{\text{Ai}'(\xi_0) \int_{\xi_0}^{\infty} \text{Ai}(q) dq}{(1 + \alpha^2) \text{Ai}(\xi_0)^2} \right\} g^*; \tag{4.22}$$

hence we have explicit expressions for the transformed pressure and axial and azimuthal wall shear distributions. They can be inverted for different centreline functions, $g(s, t)$. These results differ from those of Smith (1976*a*), as generalized for arbitrary functions g by Pedley (1980, §4.5), in the fact that $\xi_0 \neq 0$ because of the time-dependence of g .

We now consider a pure standing wave,

$$g(s, t) = \sin ks \cos \omega t = \frac{1}{4i} (e^{i(ks-\omega t)} + e^{i(ks+\omega t)}) + \text{c.c.} \tag{4.23}$$

where c.c. means complex conjugate and $k > 0, \omega > 0$. This gives

$$g^* = \frac{\pi^2}{i} (\delta(\alpha - k)\delta(\gamma + \omega) + \delta(\alpha - k)\delta(\gamma - \omega) - \delta(\alpha + k)\delta(\gamma - \omega) - \delta(\alpha + k)\delta(\gamma + \omega)) \tag{4.24}$$

and on inversion of the pressure and wall shears we obtain

$$P = \left(\frac{\Delta^{5/3}}{4i} (1 + k^2)^{-1} \left[\text{Ai}'(-\xi_0) \left(\int_{-\xi_0}^{\infty} \text{Ai}(q) dq \right)^{-1} e^{i(ks-\omega t)} + \text{Ai}'(\xi_0) \left(\int_{\xi_0}^{\infty} \text{Ai}(q) dq \right)^{-1} e^{i(ks+\omega t)} \right] + \text{c.c.} \right) b \cos \theta, \tag{4.25}$$

$$V_Y|_{Y=0} = \left(\frac{\Delta^{4/3}}{4i} (1 + k^2)^{-1} \left[\frac{\text{Ai}'(-\xi_0)}{\text{Ai}(-\xi_0)} e^{i(ks-\omega t)} + \frac{\text{Ai}'(\xi_0)}{\text{Ai}(\xi_0)} e^{i(ks+\omega t)} \right] + \text{c.c.} \right) b \sin \theta, \tag{4.26}$$

$$W_Y|_{Y=0} = \frac{1}{2} - \left(\frac{\Delta^{1/3}}{8i} \left[\frac{\text{Ai}(-\xi_0)}{\int_{-\xi_0}^{\infty} \text{Ai}(q) dq} \left\{ 1 + \frac{\text{Ai}'(-\xi_0) \int_{-\xi_0}^{\infty} \text{Ai}(q) dq}{(1 + k^2) \text{Ai}(-\xi_0)^2} \right\} e^{i(ks-\omega t)} + \frac{\text{Ai}(\xi_0)}{\int_{\xi_0}^{\infty} \text{Ai}(q) dq} \left\{ 1 + \frac{\text{Ai}'(\xi_0) \int_{\xi_0}^{\infty} \text{Ai}(q) dq}{(1 + k^2) \text{Ai}(\xi_0)^2} \right\} e^{i(ks+\omega t)} \right] + \text{c.c.} \right) b \cos \theta, \tag{4.27}$$

where now $\Delta = \frac{1}{2} ik$ and $\xi_0 = i\omega \Delta^{-\frac{2}{3}}$.

4.3. Results and discussion

The above expressions have been evaluated numerically for various values of k and ω and compared with asymptotic results for $|\xi_0| \rightarrow 0$ and $|\xi_0| \rightarrow \infty$. The numerical scheme is a fourth-order Runge-Kutta scheme with variable step size, with the values of the Airy function and its derivatives found using the NAG routine s17d_{gf}. These

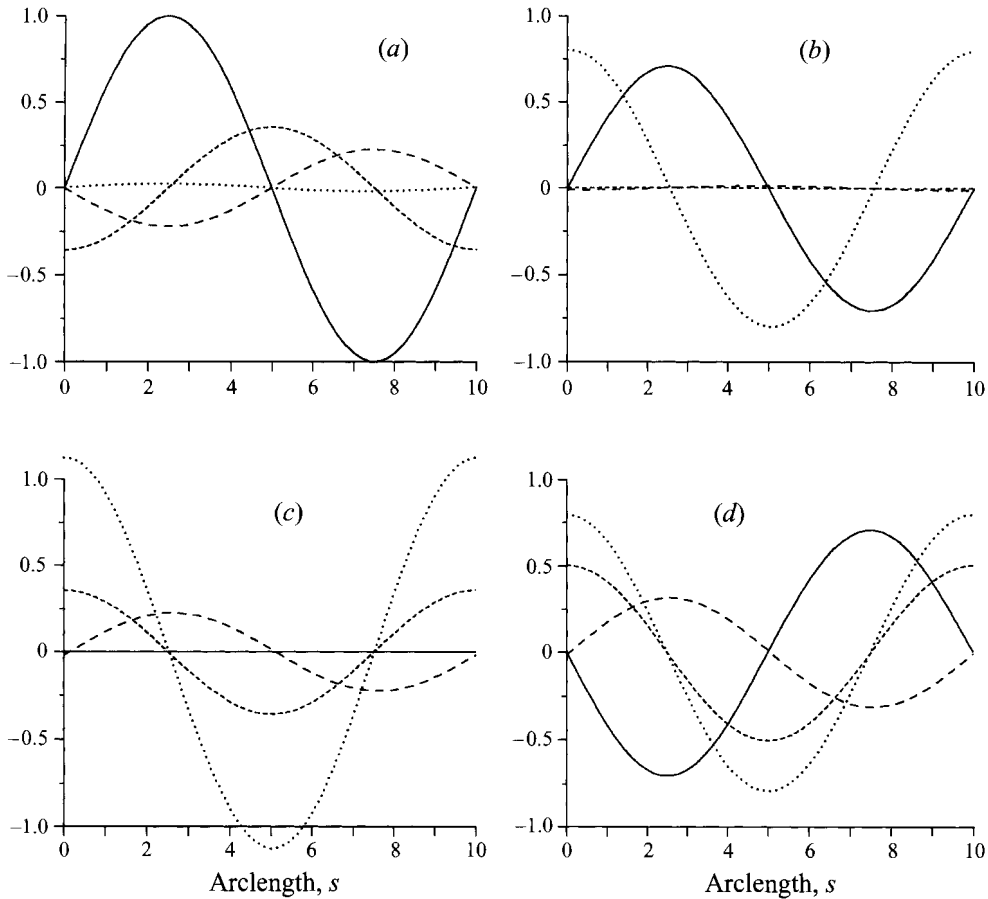


FIGURE 5. Graphs of dimensionless centreline shape (—), axial wall shear rate (---), azimuthal wall shear rate (- · - · -) and pressure (·····) for $k = \pi/5, \omega = 5, |\xi_0| \approx 10.82$: (a) $\omega t = 0$, (b) $\omega t = \pi/4$, (c) $\omega t = \pi/2$, (d) $\omega t = 3\pi/4$.

results can be seen in figures 5, 6 and 7. Since the wall shears and pressure are a combination of sine waves, values for $\omega t > \pi$ are given by $P(\omega t) = -P(\omega t - \pi)$.

For high values of $|\xi_0|$ ($k = \pi/5, \omega = 5, |\xi_0| \approx 10.82$; figure 5) we see that all three quantities vary approximately as standing waves. It can be seen that the pressure leads the centreline displacement by around $\pi/2$ in ks and lags behind by about $\pi/2$ in ωt . This means that it is maximum when $ks = 0$ and $\omega t = \pi/2$, i.e. when the centreline is straight and where the point of maximum centreline gradient would normally be. It is zero when the centreline is most curved. The azimuthal wall shear stress lags $\pi/2$ behind in ks and leads the centreline displacement by $\pi/4$ in ωt . This means that it is maximum when $ks = 0$ and $\omega t = 3\pi/4$, i.e. when the centreline is becoming most curved and at the point of maximum centreline gradient. Finally, the axial wall shear stress perturbation is out of phase (by π) in ks and leads by $\pi/4$ in ωt . This means that it is maximum when $ks = \pi/2$ and $\omega t = 3\pi/4$, i.e. when the centreline is becoming most curved and where g is at its minimum value. Both the shear stress contributions are zero when the centreline is becoming flat. These results agree with the $|\xi_0| \rightarrow \infty$ asymptotic results which are as follows:

$$P \rightarrow \frac{1}{2}k(1+k^2)^{-1}\omega \sin\left(ks + \frac{1}{2}\pi\right) \cos\left(\omega t - \frac{1}{2}\pi\right) b \cos\theta, \quad (4.28)$$

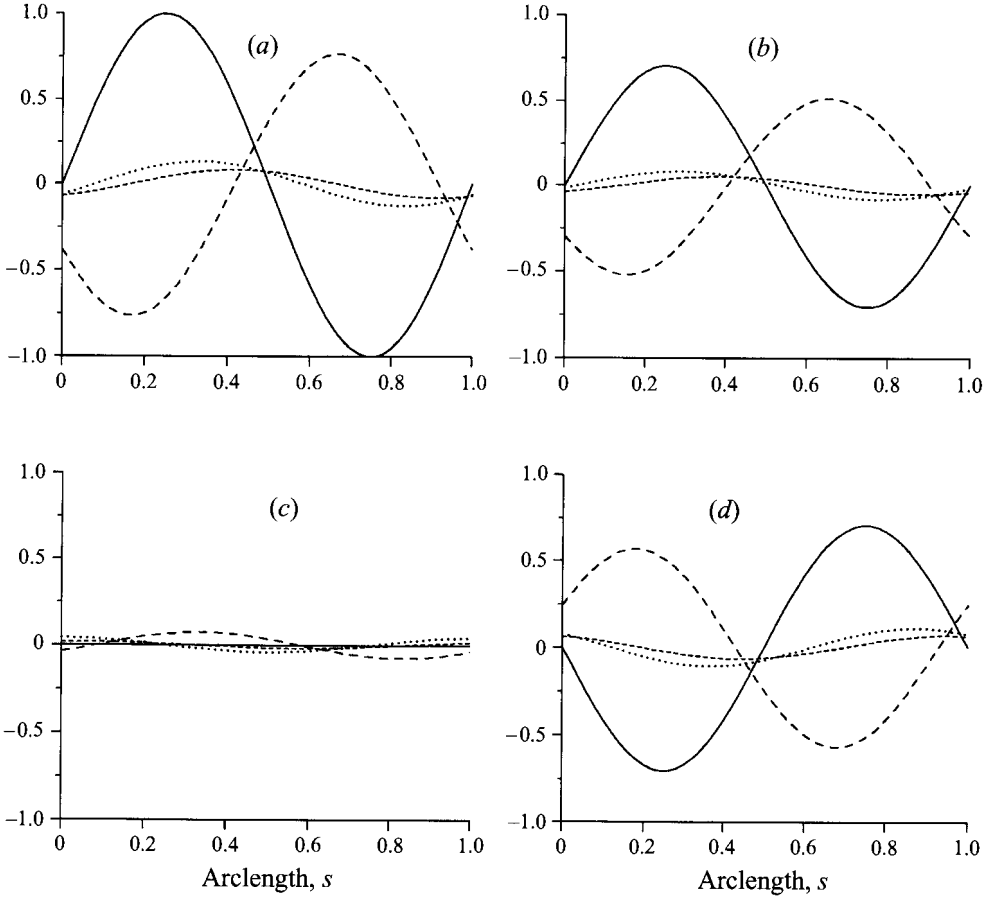


FIGURE 6. As for figure 5, with $k = 2\pi$, $\omega = \pi/5$, $|\xi_0| \approx 0.293$.

$$V_Y|_{Y=0} \rightarrow \frac{1}{2}k(1+k^2)^{-1}\omega^{\frac{1}{2}}\sin\left(ks - \frac{1}{2}\pi\right)\cos\left(\omega t + \frac{1}{4}\pi\right) b \sin\theta, \quad (4.29)$$

$$W_Y|_{Y=0} - \frac{1}{2} \rightarrow \frac{1}{2}k^2(1+k^2)^{-1}\omega^{1/2}\sin(ks + \pi)\cos\left(\omega t + \frac{1}{4}\pi\right) b \cos\theta. \quad (4.30)$$

For low values of $|\xi_0|$ ($k = 2\pi$, $\omega = \pi/5$, $|\xi_0| \approx 0.293$; figure 6) we again have approximately standing waves, but the phase differences have changed. All three computed quantities are temporally in phase with the centreline displacement, but not spatially: the pressure, azimuthal and axial wall shear stress lag by around $\pi/6$, $\pi/3$ and $5\pi/6$ respectively. These results agree with the $|\xi_0| \rightarrow 0$ asymptotic results:

$$P \rightarrow 3c_2 2^{-5/3} k^{5/3} (1+k^2)^{-1} \sin\left(ks - \frac{1}{6}\pi\right) \cos(\omega t) b \cos\theta, \quad (4.31)$$

$$V_Y|_{Y=0} \rightarrow 2^{-4/3} \frac{c_2}{c_1} k^{4/3} (1+k^2)^{-1} \sin\left(ks - \frac{1}{3}\pi\right) \cos(\omega t) b \sin\theta, \quad (4.32)$$

$$W_Y|_{Y=0} - \frac{1}{2} \rightarrow 3c_1 2^{-4/3} k^{1/3} \left(1 - \frac{c_2}{3(1+k^2)c_1^2}\right) \sin\left(ks - \frac{5}{6}\pi\right) \cos(\omega t) b \cos\theta, \quad (4.33)$$

where $c_1 = \text{Ai}(0) = 3^{-2/3}/\Gamma(2/3) \approx 0.35502$ and $c_2 = -\text{Ai}'(0) = 3^{-1/3}/\Gamma(1/3) \approx 0.25881$.

For an intermediate value we choose $|\xi_0| = 1$ ($k = 2$, $\omega = 1$; figure 7) and

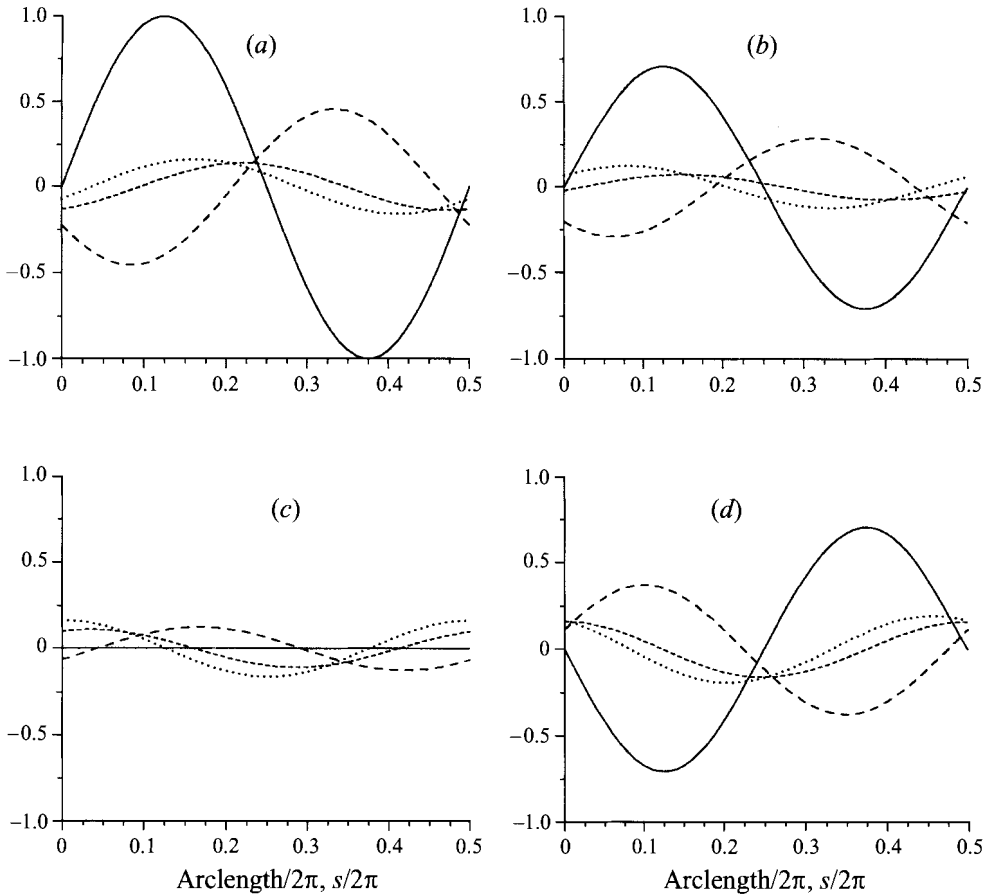


FIGURE 7. As for figure 5, with $k = 2$, $\omega = 1$, $|\zeta_0| = 1$.

find we no longer have approximate standing waves. The wall shear stress and pressure propagate in the negative s -direction. It is found that the maximum pressure occurs at $ks = 2.625$, $\omega t = -0.816$, the maximum azimuthal wall shear stress at $ks = 3.066$, $\omega t = -0.620$ and the maximum axial wall shear stress at $ks = 1.088$, $\omega t = 3.000$. The important things to notice are that the wall shear stress distributions propagate with a significant speed only when the centreline displacement is small; the values of the wall shear stress are correspondingly low then. When the centreline displacement is not small, the wall shear stress distributions do not propagate very fast and the azimuthal wall shear stress is, as before, maximum at about the point of maximum centreline gradient and the axial wall shear stress is maximum just before the inside of the bend. The pressure, on the other hand, propagates uniformly and the maximum instantaneous value stays fairly constant. Together these observations reiterate the result of maximum azimuthal wall shear stress at the points of maximum centreline gradient and maximum axial wall shear stress at the inside of bends. The results of the two previous limiting cases can be considered as a sum of the two travelling waves combining in such a way as to form a standing wave.

The above results show that even for small disturbances to Poiseuille flow, although the core flow remains effectively undisturbed, the flow within the boundary layer is substantially affected. For relatively fast oscillations the axial wall shear stress is

found to be largest on the inside of bends, i.e. when the wall is nearest the $y = 0$ line. Even for relatively slow oscillations this is found to be the case (but at a spatial phase that is $\pi/6$ ahead). This is contrary to the quasi-steady curved tube result of higher axial wall shear stress on the outside of bends. The result can be explained by continuity: the flow along the x -axis is undisturbed to the order computed so the axial wall shear stress will be greater when the wall is nearest the x -axis. For high $|\xi_0|$ the azimuthal wall shear stress is proportional to $-\phi$ (the angle the x -axis makes with the centreline), but it precedes the centreline temporally. Its effect (at $t = 0$) is to move the fluid from the inside to the outside of the bend for $0 < ks < \pi/2$, but from outside to inside for $\frac{1}{2}\pi < ks < \pi$. That is, when \hat{y}_0 is increasing/decreasing, the azimuthal velocity is negative/positive at $\theta = \frac{1}{2}\pi$, i.e. the fluid is moving towards $\theta = 0/\pi$. Finally (again for high $|\xi_0|$) the pressure is proportional to the rate of change of centreline (but preceding the centreline spatially) so that when the centreline is straight and moving at its fastest rate the pressure is at its greatest.

5. Possible application to coronary arteries

The motivation for starting this work was the desire to see the effect of overall movement on the wall shear stress distribution in human coronary arteries. Here, therefore, we estimate the actual values of the dimensionless parameters that have arisen in the two preceding sections. Whether considering major curved arteries or minor sinuous ones we have (to one significant figure):

$$\begin{aligned} \text{kinematic viscosity of blood} & \quad \nu = 4 \times 10^{-6} \text{m}^2 \text{s}^{-1}, \\ \text{period of heart beat} & \quad T \approx 1 \text{s}. \end{aligned}$$

In the case of the major arteries (§3) we may take (Sugawara *et al.* 1989, chapter 6):

$$\begin{aligned} \text{radius} & \quad a = 2 \text{ mm}, \\ \text{radius of curvature} & \quad R = 3 \text{ cm}, \\ \text{peak blood velocity} & \quad U_0 = 0.3 \text{ m s}^{-1}; \end{aligned}$$

moreover, if we assume that the volume of the left ventricle is halved during systole, then the radius of curvature will be reduced by a factor $2^{-1/3} \approx 0.8$. From this, (3.7) and (3.10) we find

$$\delta_0 \approx 0.07, \quad \epsilon \approx 0.1, \quad Re \approx 150, \quad St \approx 0.007, \quad D \approx 220. \tag{5.1}$$

The assumptions of small δ_0 , small ϵ and small St are reasonably well satisfied, although the scaling $St = O(\delta_0^{1/2})$ is not appropriate, and the additional assumption of (moderately) small D is not satisfied. For real applicability to coronary arteries future studies should extend the analysis to cover larger values of D . Note, however, that the order of magnitude of the ratios between the new terms in the wall shear stress (WSS) to the terms already known from Dean's solution, from (3.50)–(3.53) with $s = O(1)$, are

$$\begin{aligned} \text{mean axial wall shear stress:} & \quad 2 \times 10^{-7}, \\ \text{time dependent axial wall shear stress:} & \quad 9 \times 10^{-4}, \\ \text{mean tangential wall shear stress:} & \quad 5 \times 10^{-7}, \\ \text{time-dependent tangential wall shear stress:} & \quad 1 \times 10^{-3}. \end{aligned}$$

Thus the main effect of the time-dependent curvature is expected to be on the tangential wall shear stress, but even that is predicted to be rather small.

In the case of a sinuous artery (figure 1) we may take

radius	$a = 1 \text{ mm},$
wavelength	$\frac{2\pi a}{k} = 8 \text{ mm (so } k \approx 0.8),$
amplitude	$\epsilon a = 2 \text{ mm},$
mean blood velocity	$U_0 = 0.1 \text{ m s}^{-1}.$

Thus $Re \approx 25$, which is not very large as assumed; $\epsilon \approx 2$, which is not small; and $St (\approx 0.01)$ is not $O(\epsilon)$. Thus the assumptions of §4 are not satisfied. Nevertheless, we can see what the linearized theory of that section gives for $\omega = 2\pi$ and $k = 0.8$. This is a case of large $|\xi_0| (\approx 12)$ so the pressure and wall shear stress perturbations vary as standing waves and the asymptotic results of equations (4.28)–(4.30) are the most relevant. However, it is clear that different parameter ranges must be considered for genuine applicability to human coronary arteries.

The only previous studies to consider the effect of coronary artery motion on the blood flow within have been limited to the linear analysis of lateral or longitudinal acceleration of straight tubes, together with small deformation of the cross-section without change of area (Delfino, Moore & Meister 1994; Moore *et al.* 1994). Rotation and curvature were not included.

D.G.L. is grateful for financial support from EPSRC and S.L.W. from The Wellcome Trust. We would like to thank Professor W. A. Seed for letting us use figure 1.

REFERENCES

- BERGER, S. A., TALBOT, L. & YAO, L. S. 1983 Flow in curved pipes. *Ann. Rev. Fluid Mech.* **15**, 461–512.
- BLENNERHASSETT, P. 1976 Secondary motion and the diffusion in unsteady flow in a curved pipe. PhD thesis, Imperial College, London.
- COLLINS, W. M. & DENNIS, S. C. R. 1975 The steady motion of a viscous fluid in a curved tube. *Q. J. Mech. Appl. Maths* **28**, 133–156.
- DASKOPOULOS, P. & LENHOFF, A. M. 1989 Flow in curved ducts: bifurcation structure for stationary ducts. *J. Fluid Mech.* **203**, 125–148.
- DAVIES, P. F. 1995 Flow-mediated endothelial mechanotransduction. *Physiol. Rev.* **75**, 519–560.
- DEAN, W. R. 1927 Note on the motion of fluid in a curved pipe. *Phil. Mag.* (7) **4**, 208–223.
- DEAN, W. R. 1928 The stream-line motion of fluid in a curved pipe. *Phil. Mag.* (7), **5**, 673–695.
- DELFINO, A., MOORE, J. E. & MEISTER, J.-J. 1994 Lateral deformation and movement effects on flow through distensible tube models of blood vessels. *Biorheology* **31**, 533–547.
- FRIEDMAN, M. H. 1993 Arteriosclerosis research using vascular flow models: from 2D branches to compliant replicas. *J. Biomech. Engng* **115**, 595–601.
- GIDDENS, D. P., ZARINS, C. K. & GLAGOV, S. 1993 The role of fluid mechanics in the localization and detection of Atherosclerosis. *J. Biomech. Engng* **115**, 588–594.
- INABA, T. & MURATA, S. 1978 Pulsating laminar flow in a sinusoidally curved pipe. *Bull. JSME* **21**, 832–839.
- LYNE, W. H. 1971 Unsteady viscous flow in a curved pipe. *J. Fluid Mech.* **45**, 13–31.
- MCCONALOGUE, D. J. & SRIVASTAVA, R. S. 1968 Motion of a fluid in a curved tube. *Proc. R. Soc. Lond. A* **307**, 37–53.
- MOORE, J. E., GUGGENHEIM, N., DELFINO, A., DORIOU, P.-A., DORSAZ, P.-A., RUTISHAUSER, W. & MEISTER, J.-J. 1994 Preliminary analysis of the effects of blood vessel movement on blood flow patterns in the coronary arteries. *J. Biomech. Engng* **116**, 302–306.
- MURATA, S., MIYAKE, Y. & INABA, T. 1976 Laminar flow in a curved pipe with varying curvature. *J. Fluid Mech.* **73**, 735–752.
- PAO, Y. C., LU, J. T. & RITMAN, E. L. 1992 Bending and twisting of an in vivo coronary artery at a bifurcation. *J. Biomech.* **25**, 287–295.
- PEDLEY, T. J. 1980 *The Fluid Mechanics of Large Blood Vessels*. Cambridge University Press.

- PEDLEY, T. J. 1995 High Reynolds number flow in tubes of complex geometry with application to wall shear stress in arteries. *Biological Fluid Dynamics*, SEB Symp. 49 (ed. C. P. Ellington & T. J. Pedley), London, Company of Biologists.
- SINGH, M. P. 1974 Entry flow in a curved pipe. *J. Fluid Mech.* **65**, 517–539.
- SMITH, F. T. 1975 Pulsatile flow in curved pipes. *J. Fluid Mech.* **71**, 15–42.
- SMITH, F. T. 1976a Fluid flow into a curved pipe. *Proc. R. Soc. Lond. A* **351**, 71–87.
- SMITH, F. T. 1976b Pipeflows distorted by a non-symmetric indentation or branching. *Mathematika* **23**, 62–83.
- SUGAWARA, M., KAJIYA, F., KITABATAKE, A. & MATSUO, H. 1989 *Blood Flow in the Heart and Large Vessels*. Springer.
- YANASE, S., GOTO, N. & YAMAMOTO, K. 1989 Dual solutions of the flow through a curved tube. *Fluid Dyn.Res.* **5**, 191–201.
- YAO, L. S. & BERGER, S. A. 1975 Entry flow in a curved pipe. *J. Fluid Mech.* **67**, 177–196.